Advanced Bionics 1 (2025) 92–112

Contents lists available at ScienceDirect

Advanced Bionics

journal homepage: www.keaipublishing.com/en/journals/advanced-bionics/

Addressing bacterial threats in a post-antibiotic era: Bioinspired strategies for antibacterial surface design

Jiteng Zhang[a,1], Yuxiang Chen[a,1,2], Shuo Du[b,*], Mingyang Du[a], Hoon Eui Jeong[c], Rujian Jiang[b,*], Jie Zhao[a,*], Luquan Ren[a]

[a] Key Laboratory of Bionic Engineering, Ministry of Education, Jilin University, Changchun 130022, China
[b] School of Chemistry and Pharmaceutical Engineering, Science and Technology Innovation Center, Shandong First Medical University & Shandong Academy of Medical Sciences, Jinan 250117, China
[c] Department of Mechanical Engineering, Ulsan National Institute of Science and Technology (UNIST), Ulsan 44919, Republic of Korea

ARTICLE INFO

Keywords:
Antimicrobial resistance
Bioinspired antibacterial surfaces
Anti-adhesion
Mechano-bactericidal
Antibiotic-free

ABSTRACT

The advent of antibiotics revolutionized the management of bacterial infections, yet their clinical efficacy is catastrophically undermined by the global emergence of antimicrobial resistance (AMR). Furthermore, the situation is aggravated by the fact that the formation of bacterial biofilm on material surfaces significantly enhances their tolerance to antibiotics. Therefore, there is an urgent need for new approaches that employ antibacterial mechanisms distinct from those of conventional antibiotics to mitigate the risk of AMR. Recently, naturally occurring surfaces found on typical plants and insects that take advantage of physical topography can either inhibit bacterial adhesion or directly inactivate bacterial cells, showing innovative "outside-the-box" prospects for antibacterial applications and garnering considerable interest due to their drug-free nature. Bioinspired micro-/nanostructures that mimic natural surface patterns have been replicated on various biomaterials to enhance their antibacterial properties. This review summarizes and explains the current advances in bioinspired antibacterial surfaces, as well as the underlying mechanisms of various strategies. Subsequently, synergistic antimicrobial surfaces, comprising a combination of various physical antibacterial strategies, are reviewed to highlight their potential for highly efficient disinfection and long-lasting antibacterial performance. Finally, the biomedical applications, coupled with the future challenges of bio-inspired antibacterial strategies, were further discussed. We hope this review could provide valuable insights for developing innovative, antibiotic-free antibacterial strategies that deliver powerful performance in combating AMR.

1. Introduction

AMR is one of the significant public health challenges, causing severe outbreaks of bacterial infection and globally substantial death [1–4]. The issue is further compounded by the formation of stubborn biofilms on various substrate surfaces, including medical devices, industrial equipment, and other critical interfaces [5–7]. Biofilms, comprising bacterial aggregates and self-generated extracellular polymeric substances (EPS), have been documented to function as both a physical barrier that impedes antibiotic penetration while promoting the development of highly resistant bacterial variants and a reservoir that facilitates persistent horizontal transfer of antibiotic resistance genes among microbial populations [8,9]. Additionally, the global economic burden attributed to biofilm formation at material surfaces has been estimated to exceed $5000 billion annually, with significant impacts spanning healthcare, agriculture, food processing, industrial manufacturing, marine industries, and sanitation [10]. In general, the developmental trajectory of mature biofilms has been extensively characterized as a four-stage sequential process: (i) initial reversible adhesion of planktonic cells, (ii) irreversible attachment of colony bacterial cells, (iii) microcolony development through cell proliferation, and (iv) EPS-mediated maturation [11–14]. Given that surface-attached bacteria serve as the primary nucleation sites for biofilm initiation, substantial research has focused on strategies to disrupt bacterial adhesion and viability during the critical phase of adhesion [15–17]. The health-related and economic effects of biofilms

* Corresponding authors.
E-mail addresses: sdu@sdfmu.edu.cn (S. Du), jiangrujian@sdfmu.edu.cn (R. Jiang), jiezhao@jlu.edu.cn (J. Zhao).
[1] These authors contributed equally: Jiteng Zhang, and Yuxiang Chen.
[2] Current address: Department of Mechanical Engineering, The University of Hong Kong, Hong Kong SAR 999077, China.

https://doi.org/10.1016/j.abs.2025.06.001
Received 21 April 2025; Received in revised form 13 June 2025; Accepted 17 June 2025
Available online 19 June 2025

necessitate the development of effective strategies to mitigate the initial bacterial attachment at an early stage. Over the past few decades, antibacterial coatings incorporating chemical bactericidal agents, such as antibiotics, antimicrobial peptides, quaternary ammonium compounds, and metallic nanoparticles, which can interfere with the interactions between the bacteria and material surfaces, have been intensively studied and have achieved significant progress in antibacterial applications [18–20]. However, these so-called bactericidal surfaces are typically accompanied by different types of toxicity, including cytotoxicity, nanotoxicity, and nephrotoxicity [21–23]. Furthermore, emerging evidence suggests that prolonged exposure to chemically functionalized bactericidal surfaces, particularly those based on antibiotics, can induce the emergence of drug-resistant bacterial strains through non-mutational mechanisms, such as Methicillin-resistant *Staphylococcus aureus* (MRSA) [24,25]. Therefore, the focal point of antibacterial surfaces has shifted to exploring strategies to develop bactericidal surfaces with high-efficiency sterilization capability without either eliciting collateral damage to non-target mammalian cells or causing the emergence of AMR.

Throughout evolution, biological organisms have evolved defense mechanisms against environmental threats. In the case of microbial attachment, natural surface architectures with engineered micro- and nano-topographical features have been developed to physically block bacterial adhesion or exhibit mechano-bactericidal effects [26–29]. For anti-adhesion properties, natural selection has created a variety of efficient self-cleaning mechanisms for different surfaces, such as lotus leaves, fish scales, and pitcher plants, offering abundant inspiration for constructing artificial replicas [30–32]. Based on the established research consensus, the principle underlying self-cleaning performance primarily involves the naturally formed protective layer of gas or liquid phase on surfaces, which is how natural superhydrophobic, superhydrophilic, and liquid-infused surfaces operate to prevent contaminants [33–38]. For instance, the well-known “lotus effect”, characterized by superhydrophobic phenomena and self-cleaning properties, relies on the air-layer trapped by the hierarchical structures of surfaces, which serves as a cushion to prevent bacterial attachment [39–41]. Conversely, superhydrophilic surfaces, such as the fish scale, for example, which takes advantage of the affinity of water to form a thin hydration layer as a cushion layer, can also hinder the bacteria from adhering [42–44]. Consequently, these physical protective layers, including the air cushion and hydration layer, can both repel bacteria by minimizing the contact area between the substrate surfaces and bacteria, without the need for chemical agents. Additionally, of note, specific natural surfaces structured with high -aspect-ratio nanopillars were observed to physically stretch and penetrate adhered bacterial cells, exhibiting bacterial contact-killing properties [26,45,46]. The mechano-bactericidal behavior is believed to originate from the physical interaction force between nanostructures and adhered bacteria. These kinds of stresses would directly deform or damage the bacterial cell structure, compromise bacterial intracellular homeostasis, and eventually result in bacterial death [27,47,48]. Furthermore, by virtue of the advanced development of nanomaterials, this exquisite design of nature can be reproduced or mimicked artificially, offering inspiration for novel antibacterial surfaces based on entirely physical mechanisms, which could, in turn, completely circumvent the emergence of AMR.

In this review, we first summarize the promising nature-inspired and physical approaches for preventing bacterial colonization on material surfaces, focusing particularly on self-defensive strategies that hinder planktonic microorganisms from attaching and self-disinfecting strategies that eliminate adhered bacteria through intrinsic nanostructures or extrinsic physical stimulation. Subsequently, the research progress and clinical potential of synergistic physical and bioinspired antibacterial techniques are summarized and identified in the following sections, such as (i) antibacterial surfaces that combine bioinspired anti-adhesion strategies and mechano-bactericidal capabilities and (ii) self-disinfecting bactericidal surfaces that utilize multiple physical fields such as electrical fields and optical fields to enhance the intrinsic bioinspired mechano-bactericidal efficiency, achieving long-term and broad-spectrum sterilization. Overall, this article encourages researchers to reconsider the existing reliance on chemically based antibacterial coatings due to their inherent limitations. The implementation of antibiotic-free bioinspired physical antibacterial methods represents not simply an alternative strategy but a fundamentally distinct and promising paradigm that excels in green sustainability, biocompatibility, broad-spectrum efficacy, long-term capacity, and the prevention of triggering antibiotic resistance. All these innovative approaches hold transformative potential across diverse fields and applications, including nosocomial environments, medical implants, dental orthodontic treatments, personal protective equipment (PPE), and food preservation (Scheme 1).

2. Bioinspired self-defensive anti-adhesion surfaces

Bacterial adhesion and the subsequent biofilm formation represent substantial challenges in effectively treating material surface infections. Such an issue is particularly severe for implantable and indwelling devices, where it can seriously compromise the success and validity of implantation [15,49,50]. This process is fundamentally driven by physicochemical interactions between bacteria and substrate surfaces. Rather than permanently remaining in the planktonic state, bacterial cells tend to approach and adhere to material surfaces through non-specific interactions (Coulomb force, Van der Waals force, electrostatic forces, and hydrogen bonding), all of which are intrinsically governed by surface features, including hydrophobicity, nanotopography, and other factors. These initial attachments ultimately mature into irreversible biofilms, facilitating bacterial dispersal to new generations (Fig. 1a) [13,51–54]. Consequently, by modifying the surface properties such as wettability and topography, the dynamic “planktonic-or-adhering” preference of bacteria could be directly influenced. Bioinspired anti-adhesion strategies leveraging surface modifications have emerged as novel approaches to mitigate this challenge.

Natural surfaces such as lotus leaves and shark skin have been discovered to possess excellent repellency against bacterial adhesion, and their mechanisms are primarily related to their superwettability or unique microscale topographic patterns [55,56]. As one of the salient features of a solid surface, wettability significantly impacts the preference for bacterial attachment. By comparing the bacterial coverage on surfaces with varied wettability, extreme wetting conditions, such as superhydrophobic and superhydrophilic surfaces, display pronounced results in resisting bacterial adhesion, whereas moderate wetting conditions, like hydrophobic or hydrophilic surfaces, readily allow planktonic bacterial cells to colonize [57]. Along with the slippery liquid-infused porous surfaces (SLIPS) of pitcher plants, they act as another effective anti-adhesion paradigm by incorporating a second liquid. These anti-biofouling mechanisms universally operate through a protective interfacial barrier composed of entrapped air, hydration layers, or infused liquids that form between the surface and the surrounding medium. The actual contact area between the bacterial cells and substrates would be significantly diminished, thereby inhibiting the possibility of bacterial adhesion as well as the subsequent proliferation [33]. Moreover, surface topography, coupled with roughness, is another fundamental factor influencing bacterial adhesion worthy of discussion. In this section, we will highlight the advances in bioinspired strategies of superwettability systems and progress in surface topography investigation in recent years.

2.1. Superhydrophobic surfaces with entrapped air-layer

Inspired by the self-cleaning and the water-repellency of lotus leaf surfaces, the concept of superhydrophobicity has been proposed to describe surfaces with extreme exclusivity to water droplets (high water contact angles (WCA $\geq$ 150°), low sliding angles (SA $\leq$ 5°) (Fig. 1b) or

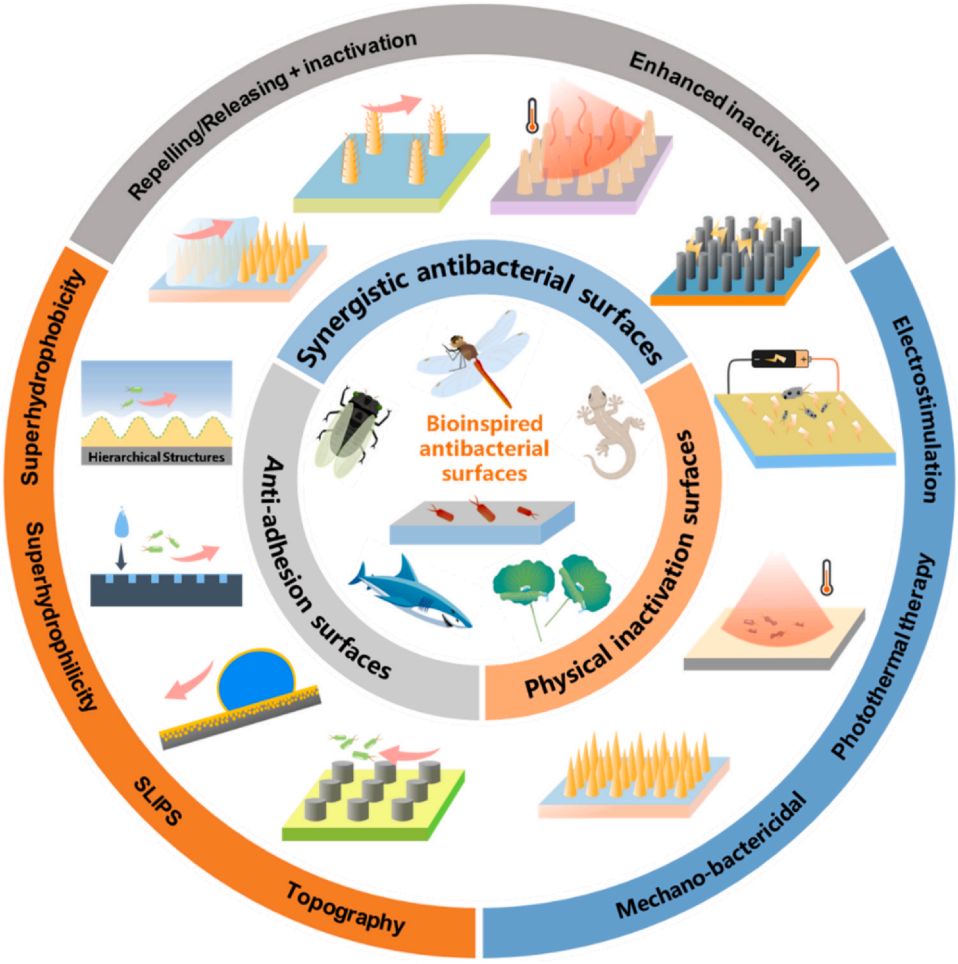

Scheme 1. Summary of current bioinspired (physical) antibacterial surfaces.

low WCA hysteresis (≤ 10°)) [58,59]. Due to the extreme affinity to air and repellency to water, an air-layer would be readily entrapped between the liquid and the superhydrophobic substrate once contacting water droplets or under submerged conditions, achieving a Cassie-Baxter wetting state (Fig. 1c). The planktonic bacterial cells, either in the water droplet or a contaminated bulk liquid environment, are thus incapable of penetrating the air-water interface owing to the high interfacial tension of water, resulting in bacterial adhesion failure [33].

To prepare a superhydrophobic surface with such bacteria-repelling capability, low surface energy, and high surface roughness are simultaneously required [60]. Generally, the popular and feasible preparation protocols can be categorized into the following two approaches: (i) Endowing common hydrophobic polymers, such as polytetrafluoroethylene (PTFE) [61], polypropylene (PP) [62,63], polydimethylsiloxane (PDMS) [64], and polycarbonate (PC) [65,66] with increased surface roughness; (ii) Reducing the surface energy of surfaces (generally are superhydrophilic surfaces) with certain degree of roughness by depositing or coating low surface energy materials like fluorochemicals or silicones (Fig. 1d) [67–70]. For instance, Pan et al. built a superhydrophobic anti-adhesion surface by constructing micro-/nano hierarchical structures and chemical surface modification (Fig. 1e). The laser-prepared micro-nanoscale cross-groove offered surface roughness, and the stearic acid surface treatment enabled the superhydrophobic properties (Fig. 1f). By adjusting the laser scanning parameters (time and spacing), the maximum WCA of 163 ± 2.5° and minimum SA of 0.5° were achieved. Regarding the antibacterial properties, three types of surfaces (polished surface, superhydrophilic surface, and superhydrophobic surface) were fabricated to investigate the anti-adhesion performance. Almost no bacterial adhesion (*Staphylococcus aureus* (*S. aureus*) and *Escherichia coli* (*E. coli*)) could be observed on the superhydrophobic surface under a stationary state. Around 99 % of *E. coli* and 93 % of *S. aureus* were hindered from attachment, which was much more effective compared to the polished surface and superhydrophilic surface [71]. Such bacteria-repelling property offers a novel strategy for functionalizing medical device surfaces. Masks, for instance, as one of the most frequently used medical items during the COVID-19 period, varied antibacterial or antivirus masks were fabricated by constructing superhydrophobic outer surfaces [72–74]. Inspired by the hierarchical structures of the lotus surface, Zhong et al. developed a self-decontaminating respirator with the synergistic antibacterial strategy of superhydrophobic property and contact inactivation. Droplets would be formed after the contaminated spray contacts the mask surface and could be easily removed with slight vibrations. This dynamic behavior, based on the trapped air-layer, could directly inhibit the initial bacterial or viral attachment, along with subsequent infections. The superhydrophobic performance and the photothermal effect of graphene, alongside the silver ion release, synergistically promote this PPE against bacterial and SARS-CoV-2 viruses [75].

Considering the inherent limitations in easy fabrication and mechanical robustness influencing critical antibacterial applications, current research efforts on anti-biofouling superhydrophobic coatings are primarily directed towards simplifying manufacturing [76–79] and enhancing functional durability [80–82]. Regarding easy fabrication, Zhao et al. proposed a highly effective dental care approach by spraying protective agents to form a superhydrophobic layer with exceptional transparency, thereby preventing bacterial fouling. Following a series of anti-adhesion analyses, it is observed that the tooth surfaces after spraying treatment could considerably inhibit bacterial attachment as well as protein adhesion. Since the adhesion of proteins in the oral

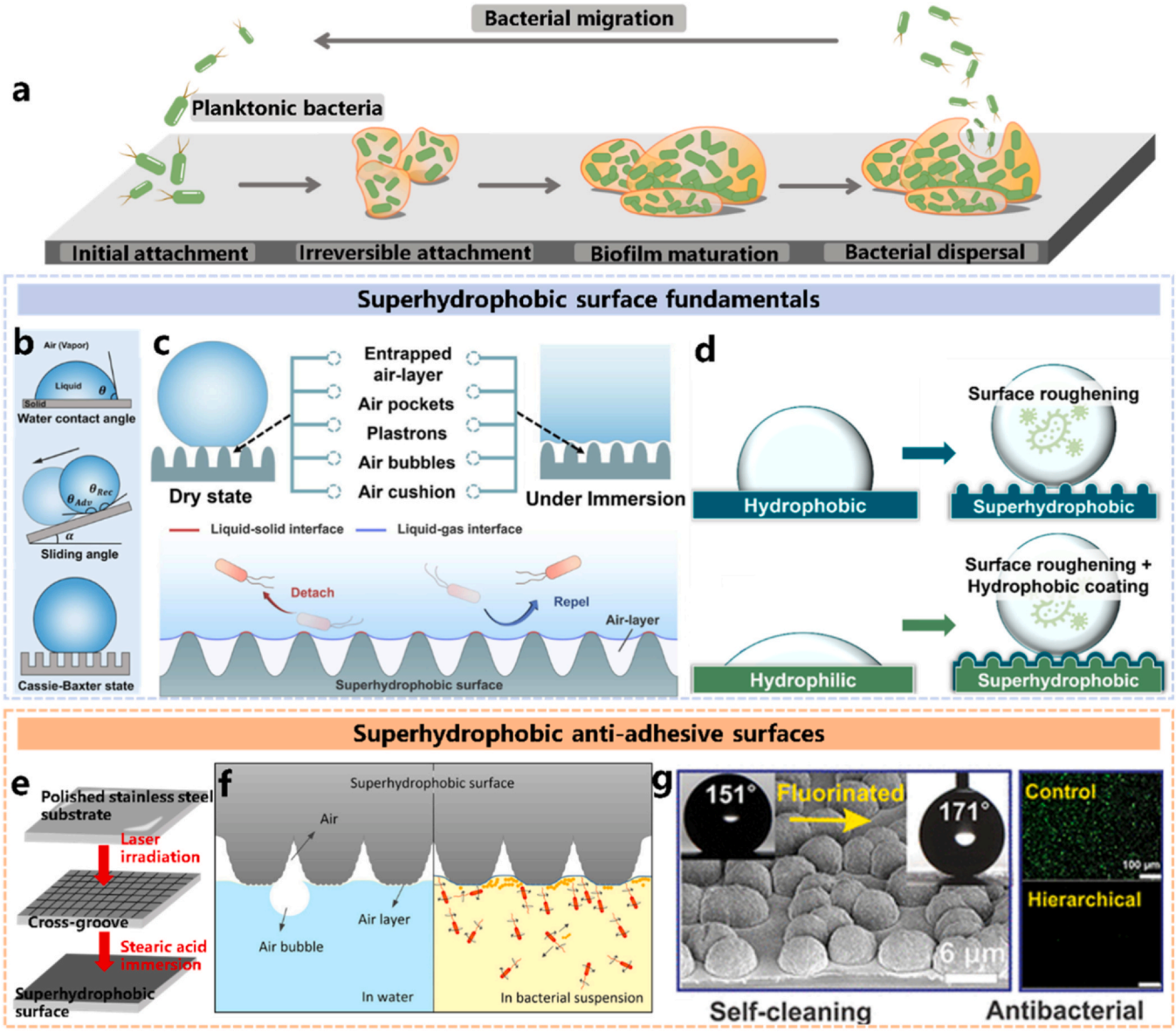

Fig. 1. Superhydrophobic surfaces and the entrapped air-layer induced anti-adhesion. (a) Schematic illustration of bacterial adhesion and biofilm formation on material surfaces. (b) Surface wettability and Cassie-Baxter state. (c) Illustration of entrapped air-layer and bacterial repellence behavior. Reproduced with permission. [33] Copyright 2023, Elsevier Ltd. (d) Possible strategies to fabricate superhydrophobic surfaces. Reproduced with permission. [60] Copyright under a Creative Commons license. (e) Schematic of hierarchical superhydrophobic surface fabrication. (f) Illustration of an air-layer captured on the superhydrophobic surface in water and anti-adhesion behavior in the bacterial suspension. Reproduced with permission. [71] Copyright 2019, Wiley Periodicals, Inc. (g) Robust superhydrophobic surface with hierarchical diamond structures and fluorescence micrographs after bacterial incubation. Reproduced with permission. [81] Copyright 2020, American Chemical Society.

cavities supplies rich nutrition and promotes bacterial growth, this sprayable coating with synergistic anti-adhesion capacity against bacterial cells and protein could present a more significant antibacterial performance [83]. For surface mechanical durability, existing research has explored diverse possible preparation methodologies, including utilizing durable materials [84], constructing hierarchical structures [85–87], and protective armors [82,88]. The underlying mechanism of the improved robustness accounts for introducing more durable or larger-scale (micron) structures to provide surface roughness, which impart extra abrasion resistance to surfaces compared to nanostructures. For instance, Wang et al. reported a biomimetic micro- and nanostructured hierarchical diamond film with outstanding hardness (Fig. 1g). This coating strategy can be widely adopted for a wide range of commercial substrates and demonstrates profound non-wetting characteristics as well as adhesion inhibition effect against bacteria (90–99 %). To illustrate the mechanical durability of this diamond superhydrophobic coating, the long-term anti-biofouling properties and hydrophobicity were examined after immersion in seawater for 28 days and sandpaper abrasion. Notably, the bacterial attachment remained greatly reduced (a 92 % reduction rate against *P. aeruginosa*), and the wettability was maintained well, indicating exceptional functional durability, corrosion protection, and mechanical wear resistance [81].

2.2. *Superhydrophilic surfaces with hydration layer*

In contrast to the significant water repellency of the superhydrophobic surfaces, superhydrophilic surfaces manifest great affinity to water, thus the liquid can completely spread out with a low static WCA $< 10^{\circ}$ [89]. Due to the extremely high surface energy and material molecular polarities alongside the surface roughness, the Wenzel

wetting state (complete liquid-solid contact) predominates over the Cassie-Baxter state (solid-liquid-vapor composite interface), resulting in superhydrophilic behavior. The hydration bond between molecules and capillary force induced by surface topography synergistically facilitates water layer retention. Therefore, the consecutive hydration layer can tightly attach to the superhydrophilic substrates [90,91], forming a barrier that inhibits the initial attachment of microbial cells.

To obtain antibacterial superhydrophilic surfaces, surface modifications, including the employment of metal inorganic compounds with intrinsic high roughness (e.g., TiO_2 nanoparticles, titanate nanotubes [92]) and utilization of hydrophilic polymers, have been widely investigated. For example, Younas et al. reported a layer of TiO_2 nanoparticles sprayed onto a polyvinylidene fluoride (PVDF)-based surface to construct hybrid membranes. Since TiO_2 considerably promotes the attraction of water molecules, the thin hydration layer can be steadily attached to the membrane surface and contributes to the pronounced bacterial adhesion resistance. The superhydrophilic membrane features almost negligible attachment of *E. coli* compared to the untreated membrane, depicting a significant anti-biofouling property [93]. In terms of hydrophilic coating polymers, such as polysaccharide [94], chitosan [95], carboxymethylcellulose [96], polyethylene glycol (PEG) [97], polydopamine (PDA) [98], polyethyleneimine [99], and zwitterionic polymers [100,101] have been extensively investigated for their proven water affinity derived from hydrogen bonding and electrostatic attraction [102,103]. Li et al. proposed an anti-biofouling coating with triblock copolymer loops consisting of mussel-inspired catechol-functionalized poly(N, N-dimethylacrylamide) (PDN) as "A" block and PEG as "B" block, forming an "ABA" spatial structure. The superhydrophilicity of PEG induced by hydrogen-bonding offered the substrate capacity to create a thin hydration layer. At the same time, PDN served as the anchors to keep the barrier layer, synergistically providing the surface anti-adhesion property. The protein adhesion reduction rate was evaluated, as the unspecific protein adhesion is a prerequisite for the following bacterial attachment. It was observed that the substrates with triblock coating exhibited a 94.4 % decrease in protein adsorption, higher than the diblock copolymer brush with "AB" structure grafted on the substrates of 86 % reduction, both of which were compared to the untreated Si substrates [104]. Unlike PEG, zwitterionic materials, containing an equal number of uniformly dispersed cationic and anionic moieties with rather high polarities, take advantage of strong electrostatic force to retain water molecules, thus forming a hydration layer [90,105]. It is reported that zwitterionic materials can exhibit a greater capacity in adsorbing water molecules than PEG due to the strong and stable electrostatic interaction, providing an enhanced superhydrophilic surface modification option [106]. For instance, Ke et al. proposed a superhydrophilic coating based on zwitterionic polymer, applied for central venous catheters (CVCs) healthcare (Fig. 2a). By pre-coating an insect-inspired phenol-polyamine film on the substrate and then grafting poly-2-methacryloyloxyethyl phosphorylcholine (pMPC), the superhydrophilic coating with a highly hydrated layer could be achieved. Researchers investigated the antibacterial performance of the pMPC-coated surface and obtained anti-adhesion rates of 99.77 ± 0.16 % and 99.58 ± 0.06 % against *E. coli* and *Staphylococcus epidermidis* (*S. epidermidis*). Moreover, the adsorption of fibrinogen and platelets was effectively hindered *in vitro*, significantly contributing to the inhibition of thrombus formation within the pMPC-modified CVCs [107].

Enlighteningly, with different constructing strategies, superhydrophilic material-based surfaces can be employed as promising candidates in several scenarios with bacterial attachment reduction

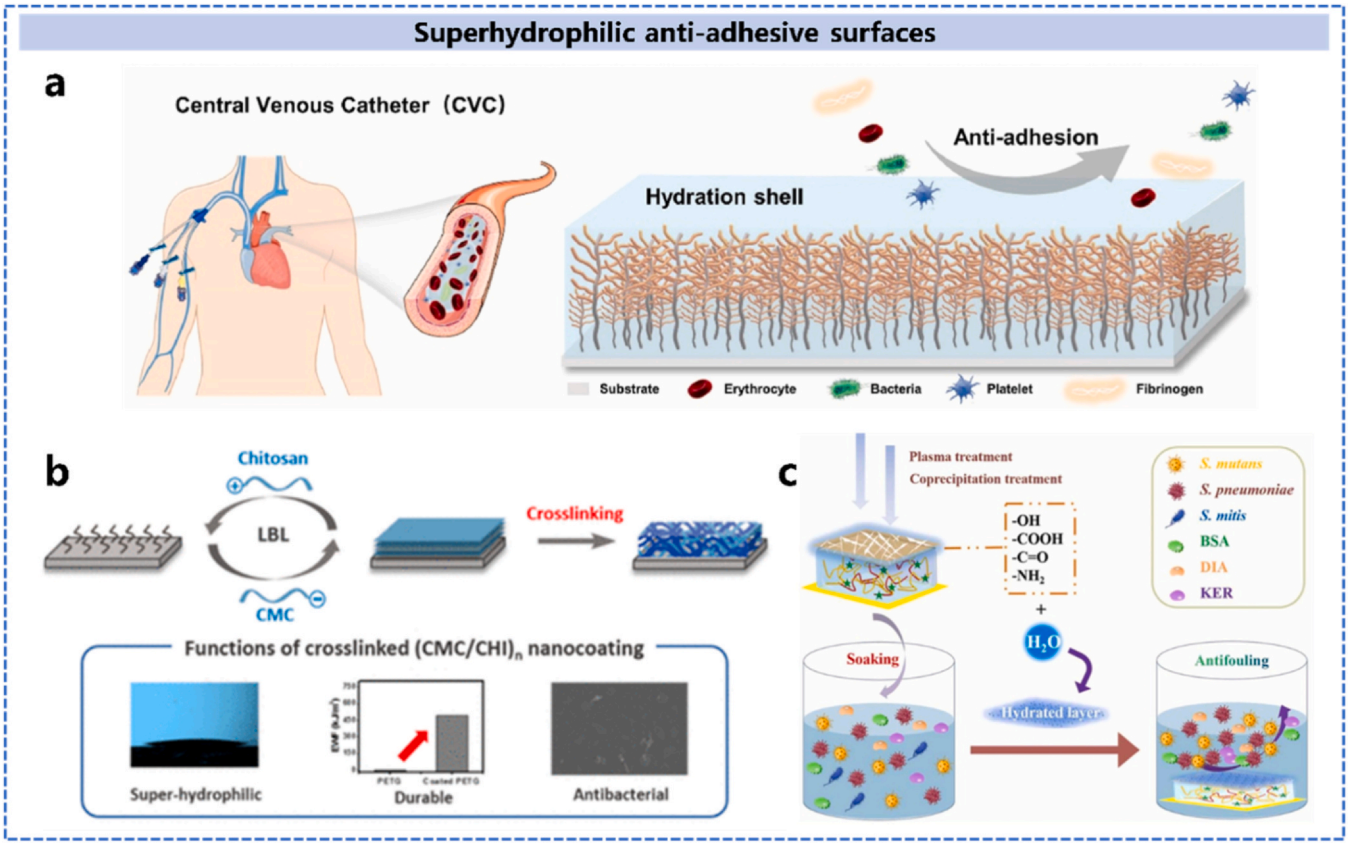

Fig. 2. Superhydrophilic surface with anti-adhesion properties. (a) Illustration of the antifouling properties of pMPC coating. Reproduced with permission. [107] Copyright 2024, the Authors. (b) Schematic of the polysaccharide-based multilayer coating fabrication and its anti-adhesion performance. Reproduced with permission. [94] Copyright 2018, American Chemical Society. (c) Illustration of antifouling behavior against bacteria and protein. Reproduced with permission. [111] Copyright 2023, Elsevier Ltd.

requirements involving orthodontic fields, orthopedic implants, ureteral stents, and ophthalmic applications [94,108,109]. Such wide biomedical applications are due to the long-term stability of the hydration layer even immersed in water, which superhydrophobic surfaces lack [110]. Relying on this advantage, Park et al. developed a superhydrophilic polysaccharide-based multilayer coating via layer-by-layer (LBL) assembly and chemical cross-linking strategies on the surface of clear overlay appliances (Fig. 2b). These appliances are frequently utilized in daily orthodontic clinics for dynamic orthodontic treatment and maintenance but have the propensity to encourage bacterial colonization. It is observed that the coating exhibited extreme water affinity (WCA $< 5^{\circ}$), and the initial bacterial adhesion was considerably reduced. *Streptococcus mutans* (*S. mutans*), the most common acidogenic oral bacteria, was used in the antibacterial test to simulate oral applications. Compared to bare surfaces covered with enormous biofilms after bacterial co-culture, the quantification of adhered bacteria on the superhydrophilic surface indicated a ~75 % anti-adhesion efficiency [94]. Another study focusing on healthcare device coating was recently proposed by Chen et al., in which researchers modified the glucose sensor with a superhydrophilic coating, endowing the device with anti-biofilm capacity (Fig. 2c). A spin coating-plasma treatment-coprecipitation treatment strategy was performed to fabricate the superhydrophilic coating on (3-Methacrylamidophenyl) boronic acid hydrogel. The superhydrophilic coating showed significant anti-adhesion effects on five different strains: *S. epidermidis*, *S. mutans*, *Streptococcus pneumoniae* (*S. pneumoniae*), *Streptococcus mitis* (*S. mitis*), and *Streptococcus oralis* (*S. oralis*), with attachment reduction of 96.3 ± 0.30 %, 98.4 ± 0.31 %, 96.8 ± 0.28 %, 99.9 ± 0.02 %, and 95.2 ± 1.18 %, respectively. Subsequent biofilm resistance tests also indicated the evident anti-adhesion property against *Streptococcus* strains (*S. pneumoniae*, *S. mitis*, and *S. oralis*) [111].

2.3. Slippery liquid-infused porous surface with oil-layer

Compared with superhydrophobic or superhydrophilic surfaces, the SLIPS that are inspired by the unique slippery surface of pitcher plants have attracted increasing attention due to their total repellence property. Taking advantage of surface microstructures, Nepenthes pitcher plants can capture moisture from the air and form a thin layer of water on their peristome. Such a water layer enables the formation of a slippery liquid surface, which effectively inhibits the possible adhesion of foulants [112]. The emerging bioinspired artificial SLIPS employing immiscible lubricants as barrier layers offer improved omniphobicity and elevated broad-spectrum antifouling efficiency compared to natural designs. In 2011, Aizenberg et al. first mimicked this natural phenomenon and introduced synthetic SLIPS. In this research, the researchers outlined three essential requirements that the constructed SLIPS must fulfill: (i) the lubricant must be stably locked within the substrate, (ii) the substrate must be wetted preferentially by the lubricant, and (iii) the lubricant layer must be immiscible with other liquids. Based on this, porous solids with micro-/nanotexture and chemically modified affinity to lubricant were prepared, covered with perfluorinated fluid serving as a lubricant, which is immiscible with both aqueous and hydrocarbon phases. Therefore, an omniphobic surface with the capacity to repel polar or non-polar liquids (water, alkanes, and blood, for example) was obtained, exhibiting superior anti-contamination performance even compared to superhydrophobic surfaces (Fig. 3a) [113]. Subsequently, Epstein et al. reported the exceptional anti-biofouling potential of such bioinspired SLIPS by investigating the adhesive behavior of biofilm matrix on them. After 48 h incubation of *P. aeruginosa* under static conditions, a uniform biofilm was seen on the control sample surface (superhydrophobic PTFE substrate). In contrast, only sparse and isolated bacterial attachment could be observed on the slippery surface (porous PTFE membrane infused with perfluoropolyether liquid). To further investigate the anti-biofilm capacity under physiologically realistic flow that approximates the varied application conditions, control PTFE samples and SLIPS surfaces were cultured with constant circulation from a peristaltic pump, which offered a 10 mL/min volumetric flow rate and 1 cm/s linear velocity. Only poorly attached microcolonies or unattached single bacterial cells could be observed on the fluorescence images, and an average *P. aeruginosa* biofilm formation reduction of 99.6 % was calculated. Moreover, two other clinically

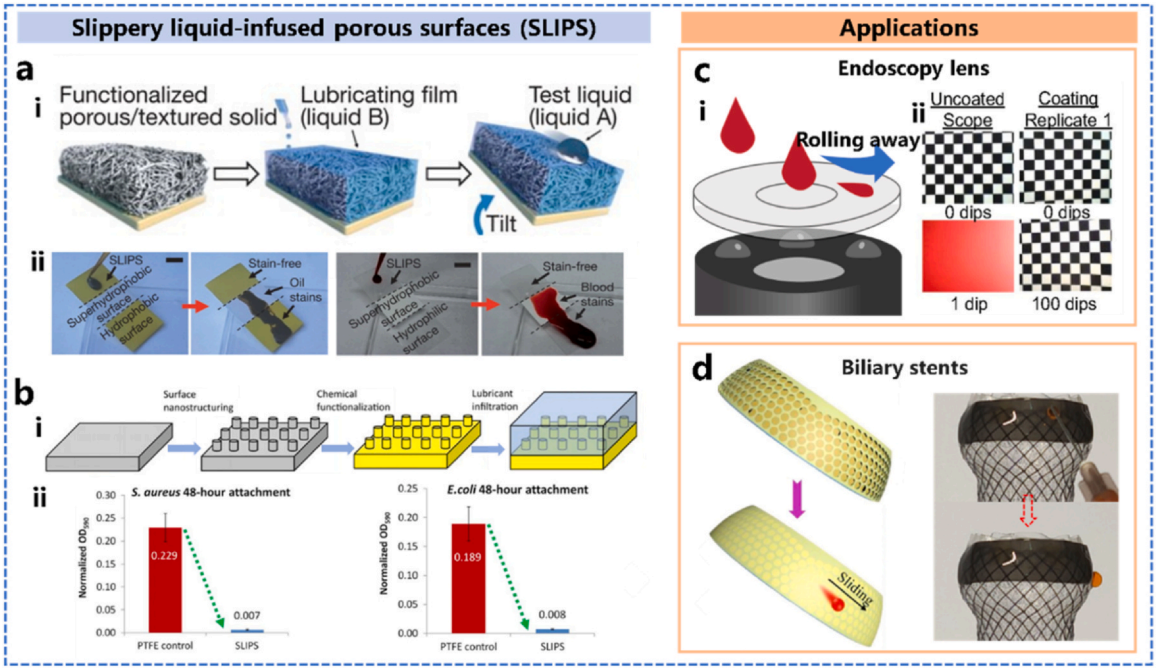

Fig. 3. Anti-adhesion SLIPS and applications. (a, i) Schematic of the bioinspired SLIPS fabrication; (a, ii) Contamination (oil and blood) repellency performance contrast of SLIPS, commercial superhydrophobic surface, and superhydrophilic surface. Reproduced with permission. [113] Copyright 2011, Springer Nature. (b, i) Illustrations of SLIPS fabrication; (b, ii) Comparison of the attachment of biofilm-forming *S. aureus* and *E. coli* of PTFE and SLIPS. Reproduced with permission. [34] (c, i) SLIPS-based endoscopy lens with antifouling properties; (c, ii) Visibility test of the lens with or without SLIPS coating in blood. Reproduced with permission. [116] (d) Schematic and picture of the anti-biofouling property of the slippery biliary stent tip surfaces. Reproduced with permission. [118] Copyright 2022, Elsevier B.V.

significant pathogenic bacteria (*S. aureus* and *E. coli*) were also studied under the abovementioned flow state. The SLIPS brought about an anti-adhesion efficiency of 97.2 % and 96 %, respectively, after 48 h, indicating the broad-spectrum antibacterial capacity against general species (Fig. 3b) [34].

Such outstanding broad-spectrum antibacterial ability and omniphobic anti-contamination of SLIPS have therefore offered promising guidance for developing effective anti-adhesion coatings in diverse medical and surgical applications [114,115]. For example, maintaining clear visibility and sterility during the endoscopic process is critical for accurate clinical diagnosis and treatment, yet long-term and frequent immersion in body fluids contributes to the non-negligible fouling by blood, proteins, cells, and bacteria. To address this challenge, Sunny et al. developed a liquid-infused glass coating coverslip on an endoscope camera lens (Fig. 3c). Through the LBL deposition, a mechanically robust porous coating was constructed on glass and subsequently infused with lubricant, obtaining SLIPS lenses with increased transparency and anti-biofouling capacities. Regarding the anti-contamination performance, the endoscope with SLIPS lens was repeatedly immersed in and out of porcine blood to estimate whether the field of view was visible. Impressively, the best sample with 10 cSt (liquid viscosity) achieved 100 % clarity even after 100 dips in blood, while the uncoated glass could barely maintain clarity after one dip. Moreover, microbial adhesion tests with *E. coli* were also carried out, demonstrating evident bacterial film reduction after 24 h, which was sufficient for short bacterial anti-adhesion [116]. Not merely restricted to building plane anti-biofouling platforms, the bioinspired liquid-infused slippery antibacterial strategy could also be adapted for interventional medical devices with curved surfaces [117]. For instance, Xu et al. developed a lubricant-infused microstructured slippery surface (Fig. 3d) based on inverse opal colloidal crystal hydrogels to render the biliary stent tip surfaces with significant anti-adhesion properties. The infused perfluorinated oil could be squeezed out when the system was heated, forming a consecutive slippery surface. After co-cultivation with *E. coli* for 24 h, the SLIPS surface was observed to have a 98.2 % anti-adhesion rate and furthermore achieved 99.0 % antibacterial efficiency through the synergistic function of antibiotics (Imipenem). Interestingly, the unique microstructures provided sufficient space for lubricants and loaded antibacterial drugs and imparted the slippery surface with tunable bioinspired structural color that could visually vary and be used to monitor the drug release process. Such work also indicates that the research trend of slippery surfaces in biomedical applications focuses on designing a dual-functional or multifunctional platform based on the liquid-infused substrate with excellent anti-adhesion properties [118].

Critical challenges hindering the widespread use of these bioinspired slippery coatings in clinical applications remain their susceptibility to lubricant depletion or mechanical damage, necessitating research on robustness modification to supplement long-term durability and antimicrobial capacity [115,119]. Regarding liquid lubricant depletion, alternative strategies through applying two-dimensional structures [120], and liquid-like slippery surfaces [121,122] offer potential solutions to reduce lubricant loss. The underlying mechanisms of stability enhancement could be summarized as follows. Introducing complex structures can significantly increase the interfacial capillary force that facilitates liquid lubricant retention and possible lubricant replenishment when depletion occurs [123,124]. Rather than relying on liquid lubricants, solid slippery surfaces with covalently grafted polymer brushes or alkyl monolayers can achieve omniphobic behavior and lossless coating degradation [125,126]. Moreover, novel strategies focusing on the comprehensive stability of SLIPS have been launched. For instance, Zhang et al. notably proposed a hierarchical SLIPS combining microscaled honeycomb-patterned microstructures (Ti-6Al-4V alloy) with nanoscaled lubricant reservoirs. Due to the introduction of the regular hexagon structures, the lubricant layer loss decreased significantly to 12.16 % even after seawater brushing for 10 days. Moreover, when the surface is under abrasion, the microstructure could first withstand the wear and keep the lubricant nano-containers on the lower surface intact, ensuring the long-term slippery property. The antibacterial assessment proved that the SLIPS could significantly reduce bacterial adhesion compared to the non-slippery surfaces, and the microscaled honeycomb array also exhibited the confining capacity of the few adhered bacteria, preventing the pathogens from transmission [127].

2.4. Surface topography

Topography, which can be evaluated by a set of standard roughness parameters (such as average roughness (R_a), root mean square (RMS) roughness (R_q), and other indicators), significantly impacts bacterial adhesion [128]. Since the first exploration of antifouling micropatterns on shark skins [129], a series of nature-mimicking patterned surfaces were explored, involving high-aspect-ratio structures, ripples [130], wells [131], grooves [132], pillars [133,134], protrusions [135], and honeycombs [136] from micro- to nanoscale. Behind these advances, surface topography, as a critical determinant of bacterial adhesion, is now harnessed to offer a strategic pathway for designing antibacterial surfaces [33,57,128,137,138]. As summarized in Fig. 4a, there are three regions in which the surface topography exhibits notable antibacterial efficiency over 50 %: (i) high-aspect-ratio nanostructures exhibiting mechano-bactericidal effect, (ii) patterned surfaces with a feature size near one μm with anti-adhesion properties, and (iii) larger-scale patterns induced selective bacterial adhesion [57]. In principle, the anti-adhesion mechanism underlying specific surface topography is mainly attributed to the maximum cell deformation of bacteria and the minimum available bacteria-substrate contact area, as a higher adhesion force can be obtained when bacteria achieve a larger accessible area [139]. It is also reported that micro-/nanostructures can hinder bacterial conjugation, a critical mechanism in horizontal gene transfer, thus circumventing the emergence of antibiotic resistance [140,141]. Furthermore, varied scales of roughness, especially the nano-roughness, play an important role in manipulating bacterial adhesion [142]. Different bacteria adhesion behaviors, therefore, could be observed on different regions of roughness.

Although no clear consensus on specific dimensions and antifouling patterns has been reached, there is a common observation that topographical patterns within the microscale (1–20 μm) could exhibit outstanding anti-adhesion properties due to the limited contact area between bacteria and surfaces [132,143,144]. In addition, it is generally believed that bacterial adhesion force is positively correlated with surfaces with submicron/micron roughness [57,139,145,146]. Microwells, for instance, have been proven to exhibit anti-adhesion capacity determined by the well diameter [136,144]. The surface with microwells (diameter ~1 μm) exhibits a trapping behavior that leads to bacterial deformation, which in turn inhibits bacterial proliferation. Such inhibition endows the surface with higher antimicrobial efficiency than other surfaces with larger micropores (~2 μm, ~4 μm) [132,136]. In another study, the air-layer retained in micropores with diameters ranging from 3.5 to 11 μm acted as an air cushion to prevent potential bacterial adhesion. However, evident pathogen settlement could be observed with a larger well diameter (> 11 μm), indicating the significance of dimension in constructing anti-adhesion surfaces [143]. Interestingly, other micron morphologies such as microgrooves and micro-protrusions not only possess anti-adhesion properties but also impede the movement of microorganisms by confining adherent bacteria to the edges of features (Fig. 4c), preventing further bacterial infection [127,147–149].

Slightly distinct from micropatterned surfaces, which rely on direct reduction of contact area, nanoscaled surfaces adapt to the molecule level of interactions to achieve anti-adhesion [150]. Studies have confirmed that the bacterial adhesion force could exhibit a conflicting correlation with roughness, making roughness-induced adhesion a key area of investigation (Fig. 4b) [57,142,151,152]. When the roughness is

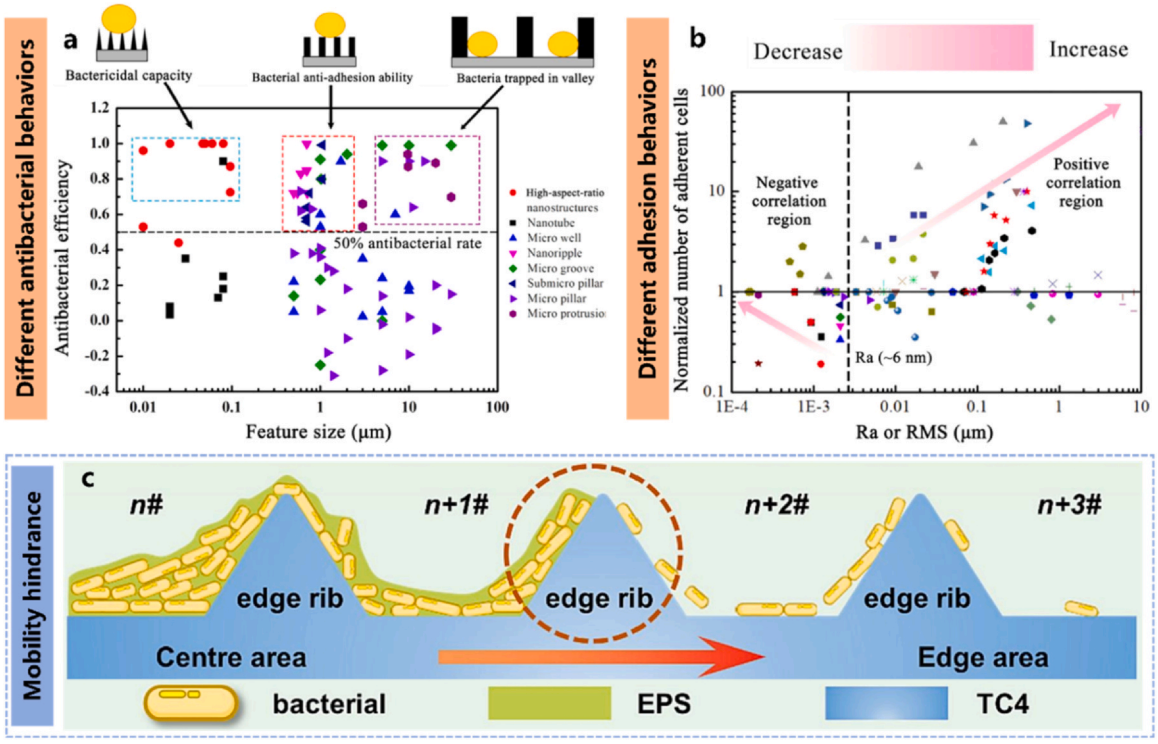

Fig. 4. Influence of surface topography and roughness on bacterial adhesion. (a) Summary of different antibacterial performance and corresponding microstructures (scale sizes and shapes). (b) Chart of negative and positive relationships between bacterial attachment and specific surface roughness region. Reproduced with permission. [57] Copyright 2022, Elsevier Ltd. (c) The ribs of microscale hexagon structures restricting the movement of *Pseudoalteromonas*. Reproduced with permission. [127] Copyright 2023, Elsevier B.V.

low (R_a < 6 nm), bacteria tend to adhere more readily to smoother surfaces under static conditions [151,153]. This tendency can be attributed to surface-mediated bacterial metabolism, such as the increased secretion of EPS on smooth surfaces, facilitating initial colonization and biofilm formation [153]. The following decrease in adhesion force with the increasing roughness is attributed to the corresponding reduction of the effective anchor points between the macromolecules on the bacterial cell wall and the surfaces [152]. As the roughness further increases (R_a 6–30 nm), bacteria exhibit a preference for adhering to rougher surfaces due to the larger surface area available for attachment [154]. Generally, with higher roughness over 6 nm, the bacterial adhesion can be identified as positively associated with surface roughness, as summarized. At the same time, many nanoscale surface features with high-aspect-ratio demonstrate lethal effects on bacteria, primarily by mechanically penetrating bacterial membranes. The detailed mechanisms and implications of these effects will be explored further in the following sections.

Apart from the effects of topography and roughness, different bacterial species demonstrate diverse accommodation preferences and adhesion behavior on various surface features [142,155]. For example, *S. aureus* preferred to attach to the microwells with a diameter of 0.5 μm, while *P. aeruginosa* preferred the smooth surface [156]. Generally, bacterial adhesion is suppressed when the dimensions of surface topographical features are smaller than the size of bacteria, whereas larger topographies tend to promote adhesion. Due to the distinguished sizes of Gram-positive and Gram-negative bacteria, a specific range of topographical parameters might only work efficiently for one species [149]. Moreover, Gram-positive and Gram-negative bacteria exhibit different sensitivity toward the alteration of surface roughness. It was revealed that Gram-negative bacteria, such as *E. coli*, exhibit a higher sensitivity when the contact surface roughness changes. In contrast, Gram-positive bacteria like *S. aureus* tend to ignore the variations [157]. Overall, the practical applications of surface topography rely on the suitability of bacteria and morphology. Different surface topographies with specific parameters or patterns should be designed according to the prominent bacterial strains and the applied environment to optimize the anti-adhesion efficiency. Customized anti-biofouling surface-modifying strategies are still in great need regarding personal infection treatment, healthcare device surface preparation, and other antifouling areas. Hopefully, the specifically designed surface topography may offer insights into the solutions to these critical situations.

3. Bioinspired self-disinfecting bactericidal surfaces

Nature has evolved sophisticated nanostructures on biological surfaces, equipping them with remarkable bactericidal capabilities to counteract potential microbial contamination [39,158–160]. Recently, the inspiration from these naturally selected prototypes and advances in the nanofabrication technologies have significantly promoted the existing comprehension of the mechano-bactericidal mechanisms and meanwhile served as constructive guidance to designing physical inactivation surfaces. This section will review the investigations of the naturally bactericidal surfaces followed by the recent progress of artificial analogs with corresponding or exceeding bactericidal properties.

3.1. Naturally selected nanostructured mechano-bactericidal surfaces

Diverse natural surfaces, such as insect wing surfaces, animal skins, and plant leaves, have revealed their mechano-bactericidal capacities [161]. Ivanova et al. initially reported the inactivation interaction between the adhered *P. aeruginosa* and the densely-arranged nanopillars on the wing surface of cicada (*Psaltoda claripennis*) (Fig. 5a). It was observed through the SEM images that the morphology of adhered bacterial cells was drastically altered as the nanopillar structures penetrated the bacterial surface. Cellular components diffused outwards where the contact between the single bacterial cell and nanopillars occurred, and the subsequent viability analysis confirmed the death

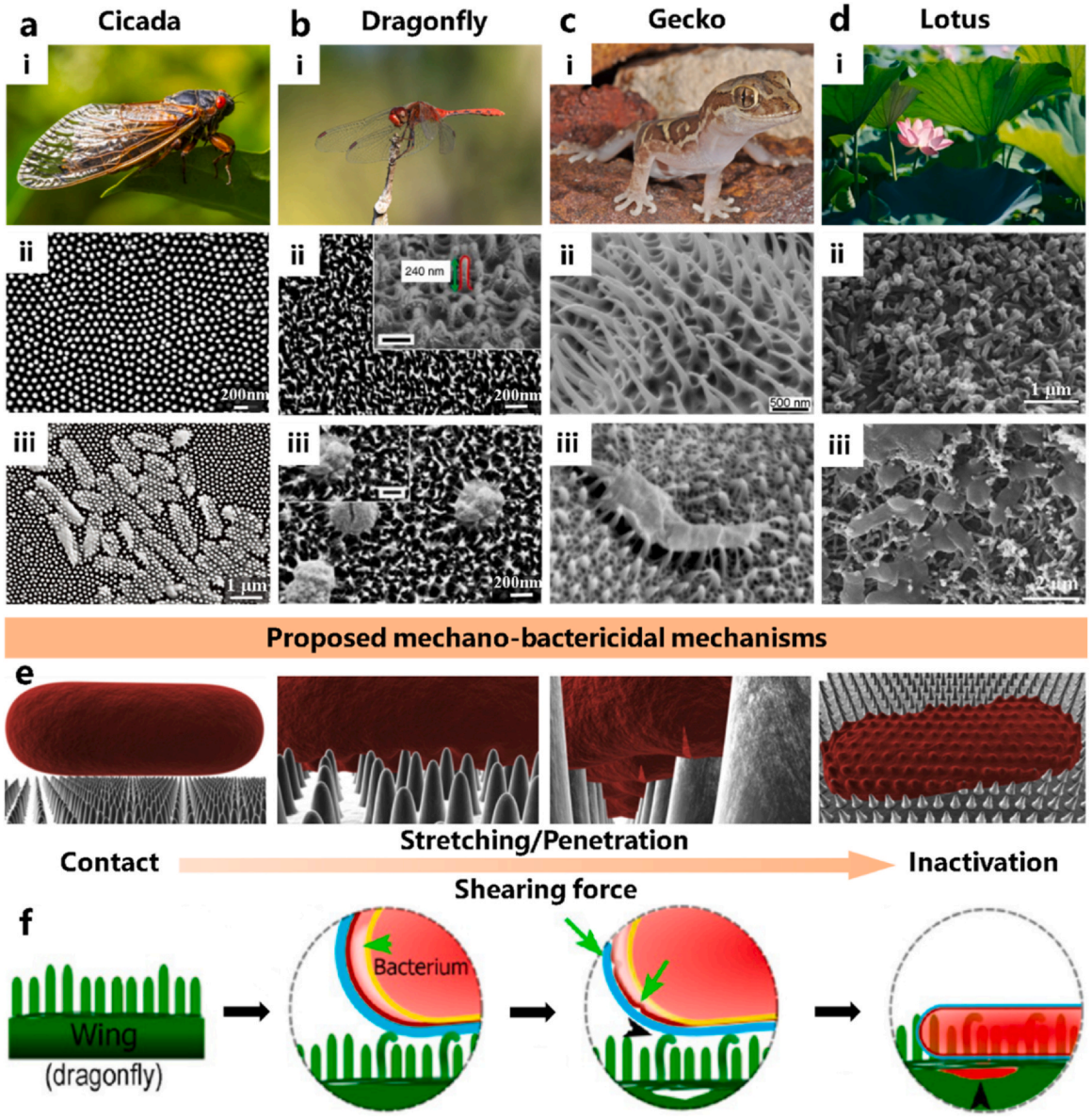

Fig. 5. Prototypes of natural bactericidal surface with high-aspect-ratio and proposed mechano-bactericidal mechanism. (a, i) Photo of living *Psaltoda claripennis*; (a, ii) natural nanopillars of the cicada wing surface. Reproduced with permission. [162] Copyright 2013, Elsevier Inc.; (a, iii) mechano-bactericidal behavior of the nanopillars. Reproduced with permission. [158] Copyright 2012, WILEY-VCH Verlag GmbH & Co. KGaA, Weinheim. (b, i) Photo of living *Diplacodes bipunctata*; (b, ii) natural nanoclusters of the dragonfly wing surface; (b, iii) mechano-bactericidal behavior of the nanoclusters. Reproduced with permission. [164] Copyright 2013, the Author(s). (c, i) Photo of living *Lucasium steindachneri*; (c, ii) natural nano-spinules of the gecko skin surface; (c, iii) mechano-bactericidal behavior of the nano-spinules. Reproduced with permission. [159] Copyright 2015, Elsevier Ltd. (d, i) Photo of *Nelumbo nucifera* leaf; (d, ii) natural hierarchical structures of lotus surface. Reproduced with permission. [259] Copyright under a Creative Commons Attribution (CC BY) License; (d, iii) mechano-bactericidal behavior of the hierarchical structures. Reproduced with permission. [168] Copyright 2020, Elsevier B.V. (e) Illustration of mechano-bactericidal effect on cicada-wing-inspired nanopillared surface, relying on stretching and penetration behavior. Reproduced with permission. [162] Copyright 2013, Elsevier Inc. (f) Illustration of another proposed mechano-bactericidal effect on the dragonfly wing surface, relying on shearing force. Reproduced with permission. [47] Copyright 2017, American Chemical Society.

state of these attached bacteria. Such sterilization phenomenon was still preserved on the cicada wing after surface chemistry alteration, suggesting that the bactericidal property is attributed to purely physical or mechanical mechanisms instead of any chemical interactions [158].

To further understand the underlying sterilization mechanism, a biophysical model of the interaction between the attached bacteria and the nanopillar structures was proposed in the following works (Fig. 5e). Upon contact with the regularly arrayed nanopillars on the cicada wing surface, the bacterial cell membrane will adsorb onto the pillar tips (Region A), leading to an increase in total membrane area. This adsorption causes the segments of bacterial membrane suspended between the pillars (Region B) with stretching behavior. The established biophysical mechanics model indicates that the Region B undergoes significantly a higher strain than Region A. As the stretching in Region B reaches a critical threshold, irreversible mechanical rupture of the membrane and consequent bacterial inactivation will occur. This entire bactericidal process is purely mechanical, driven solely by the physical nanostructure and the mechanical properties of the cell membrane, without requiring any specific biochemical interactions [162]. Furthermore, Kelleher et al. investigated the wing surface bactericidal activities among three different cicada species (*Megapomponia intermedia*, *Ayuthia spectabile*, and *Cryptotympana Aguila*) with various topography parameters, including pillar size, inter-spacing, and aspect-ratio. Fluorescence images of bacteria test verified that the mechano-

bactericidal efficiency of *Pseudomonas fluorescens* (Gram-negative bacteria) was mainly governed by the spatial parameters of nanopillars. It was found that the densely arranged array and higher aspect-ratio would contribute to higher mechano-bactericidal efficiency [163].

Dragonfly wing surfaces were also well investigated for their mechano-bactericidal capacity. Ivanova et al. characterized the *Diplacodes bipunctata* upper wing surface (Fig. 5b), obtaining nanoclusters with random sizes, shapes, and interspacing, significantly distinct from the mentioned regularly arranged surfaces. Noteworthily, the sharp and irregular nanostructures not only inactivated Gram-negative bacteria (*P. aeruginosa*) but also showed extra lethality to the Gram-positive bacteria (*S. aureus* and *Bacillus subtilis* (*B. subtilis*)) compared to the cicada wing surfaces This broad-spectrum inactivation behavior is believed to derive from the disordered hierarchical nanoclusters with bending shape, which can provide higher tearing force towards bacteria [164]. Nanomechanical modeling shows that the nanostructures of this natural prototype have a high gradient of curvature, which leads to a high downward adhesive force and increased rate of this force when penetrating. Both of these superiorities facilitate bacterial cell rupture and lysis, significantly determining the broad-spectrum bactericidal efficiency [165]. More detailed inactive behavior the of dragonfly (*Orthetrum villosovittatum*) wing surface with biphasic nanopillar array (short pillars and tall pillars disordered arranged) offers a novel mechano-bactericidal mechanism. More specifically, the nanopillars can trigger bacterial (*E.coli*) EPS secretion, forming a strong Van der Waals force-induced adhesive interface where bacteria are immobilized. When bacteria attempt movement, shear forces will induce elastic bending of tall nanopillars, transmitting asymmetric stress to the cell envelope and leading to bacterial membrane delamination (the separation of the outer membrane and inner membrane). Mechanical traction effect and local stress will be amplified as bacteria move, which results in cell rupture. After the inner membrane breaks down, bacterial cells will eventually collapse into nanostructures (Fig. 5f). This adhesion-shear synergy varies from puncture/stretching theories, with dual-height nanopillars achieving mechano-bactericidal effect through the above-mentioned cascade [47]. Likewise, the gecko (*Lucasium steindachneri*) (Fig. 5c) skin consisting of irregular nano-spinules was proven to have an eliminative function to the attached Gram-negative bacteria (*porphyromonas gingivalis*), exhibiting a significant deformation of the cell walls that resembled the adhered bacteria on the cicada wing surfaces [159]. Moreover, with similar randomly arranged nano-protrusions [166], the damselfly (*Calopteryx haemorrhoidalis*) wing surfaces were investigated to assess the mechano-bactericidal capacity towards different life stages of the pathogens. Natural surfaces adhered with *S. aureus* and *P. aeruginosa* were tested across 24 h. Bacterial growth was separated into five stages: Young (1 h), Early mature (6 h), Mature (12 h), Late mature (18 h), and Old (24 h), concluding that the bacteria of the earlier stage could be more vulnerable due to the fragility of the bacterial wall compared to the elder stage. This various susceptibility was supposed to be related to the different rigidity of the cell walls at specific physical stages, which correlated with the previous conclusion on bacterial rigidity. Notably, *S. aureus* with thicker peptidoglycan layers is less sensitive to the mechano-bactericidal effect than *P. aeruginosa*, which will be discussed in the following section [167].

Beyond these insect surfaces featuring single-tier bactericidal nanostructures, the hierarchical micro-/nanostructures on numerous plant leaf surfaces have been reported to impart superwettability and endow exceptional mechano-bactericidal capacity against attached microorganisms. For example, Jiang et al. primarily investigated the antibacterial properties of the lotus (*Nelumbo nucifera*) leaf surface by assessing the viability of the attached bacterial cells within its hybrid hierarchical micro- and nanostructures (Fig. 5d). The SEM images of the adhered *E. coli* demonstrated similar deformations to those on cicada and dragonfly wings, which had been identified as the result of external stress applied by the nanostructures. After 12 h of co-cultivation, fluorescence demonstrated that all the adhered *E. coli* were inactivated, with a minuscule surface coverage of around 3 %, further confirming the mechano-bactericidal effect and the self-cleaning property [168].

3.2. Artificially nanostructured mechano-bactericidal surfaces

As the mysteries of natural nanostructured surfaces continue to be unveiled, artificial surfaces inspired by these biological models are highly valued. Based on natural surface prototypes, artificial surfaces focus on dimensional parameter improvement and optimization, delving deeper into the underlying physical mechanisms and thereby enabling novel antibacterial applications of biomaterial surfaces.

Ivanova et al. first reported the pioneering bioinspired antibacterial surface constructed on a black silicon substrate through reactive ion etching (Fig. 6a), reproducing the dragonfly (*Diplacodes bipunctata*) wing surface nanostructures with random shapes and non-uniform spatial distribution. SEM and optical profilometry images showed the nanopillars of the artificial surface were sharper, taller, and more spatially distinct from each other compared to the natural counterparts, which therefore imparted their varied mechano-bactericidal efficiency. It was revealed from the bactericidal tests using three strains of bacteria (*P. aeruginosa*, *S. aureus*, and spores of *B. subtilis*) that the black silicon surface demonstrated a notably higher sterilization rate compared to the natural surface. Both are more effective in comparison to the cicada wing surface due to the higher stress caused by sharper nanospikes [164]. In another work, Wandiyanto et al. fabricated randomly arranged sharp nanosheets using hydrothermal etching method on Ti substrates. The asymmetrical blade-like structure could be adjusted by tailoring the hydrothermal period. Specifically, prolonged treatment leads to larger spatial features but lower density and sharpness, whereas shorter treatment results in smaller, denser, and sharper structures. The 6 h treated titanium substrate with the network of nanoflakes displayed the highest antibacterial efficiency towards both *P. aeruginosa* and *S. aureus*, up to 99 ± 3 % and 90 ± 9 %, respectively. This high fatality is attributed to the sharper and more widely spaced nanosheets, which generate higher stress onto bacterial membranes [169]. Apart from the randomly featured nanostructured surface replication, artificial surfaces with well-ordered geometry parameters were further investigated (Fig. 6b-c) [170,171]. For instance, Dickson et al. leveraged nanoimprint lithography to replicate the wing surfaces of cicada using poly (Methyl methacrylate) (PMMA) substrates. These substrates were then incubated with *E. coli* to assess their bactericidal properties. Different bioinspired surfaces were fabricated for different cycles with pitches of P200, P300, and P600, respectively, in which P200 represented the natural topography of cicada wings and the pillar interspacing is 170 nm. Antibacterial characterizations illustrated that the film with pillars could be more lethal to *E. coli*, preventing biofilm formation compared to the non-structured surface. Furthermore, the amount of dead *E. coli* on the three surfaces was evaluated, and it was concluded that the P200 with a smaller diameter (70 nm) and interspace has the highest bactericidal efficiency, indicating the significance of the structure parameters [171].

Theoretically, the cicada-wing-inspired pillared surfaces were analyzed by a quantitative thermodynamic theory regarding the adhered bacteria-free energy change (ΔE). According to the simulation, the higher ΔE represented higher mechano-bactericidal capacity, which is closely related to the cell membrane stretching modulus and surface morphology. In conclusion, the artificial surfaces consisting of nanopillars can increase their roughness to some extent by properly adjusting the distribution density, radius, and height of nanopillars to enhance their ability for contact killing [172]. For instance, Ye et al. investigated the physical inactivation of *S. aureus* on nanostructures by adjusting spatial parameters. Three types of Al_2O_3-wrapped nanorod arrays (Al_2O_3@HNRes, Al_2O_3@ZNRes, and Al_2O_3@ZNRl) with distinct top sharpness (conical angles of 180°, 50°, and 50°) and heights (~462 nm, ~469 nm, and ~884 nm) were fabricated. After 24 h of bactericidal test, Al_2O_3@ZNRes and Al_2O_3@ZNRl with shaper top

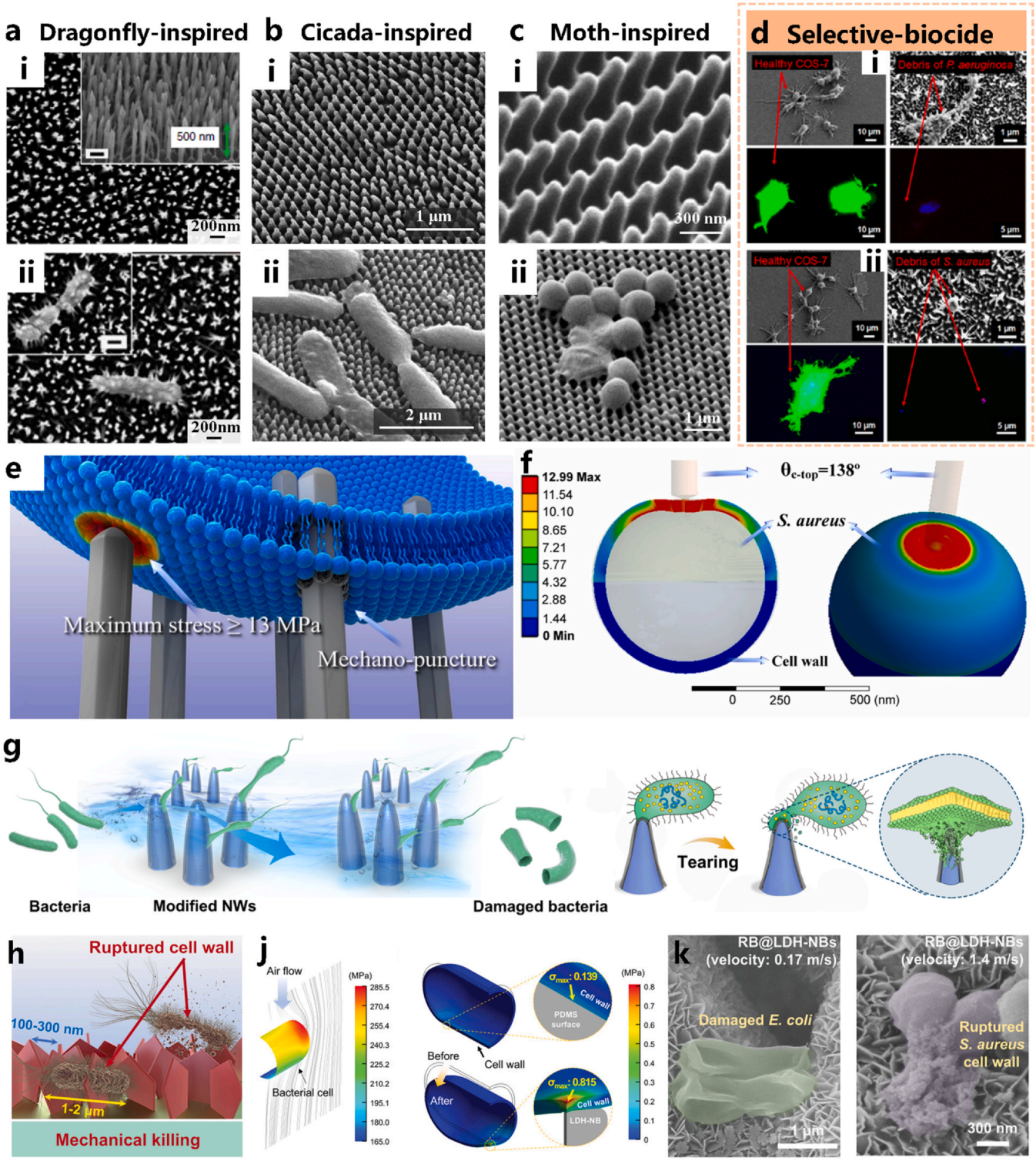

Fig. 6. Artificial mechano-bactericidal surfaces and antibacterial properties. (a, i) Black silicon surface with nanospikes inspired by dragonfly wing surface; (a, ii) mechano-bactericidal behavior of the nanospikes. Reproduced with permission. [164] Copyright 2013, the Author(s). (b, i) PMMA nanopillars inspired by cicada wing surface; (b, ii) mechano-bactericidal behavior of the nanopillars. Reproduced with permission. [171] Copyright 2015, AIP Publishing. (c, i) Moth-eye-inspired nanopillared surface; (c, ii) mechano-bactericidal behavior of the nanopillars. Reproduced with permission. [170] Copyright 2018, IOP Publishing Ltd. (d, i) Selective-biocide effect of black silicon surface towards COS-7 cells and *P. aeruginosa*; (d, ii) Selective-biocide effect of black silicon surface towards COS-7 cells and *S. aureus*. Reproduced with permission. [178] Copyright 2016, American Chemical Society. (e) Illustration of mechano-puncture with topical stress over 13 MPa. (f) FEM result of critical stress of *S. aureus* cell wall. Reproduced with permission. [173] Copyright 2021, the Authors. (g) Novel mechanism of mechano-bactericidal due to shear flow that brings bacteria to the pillars. Reproduced with permission. [174] Copyright 2023, under a Creative Commons Attribution (CC BY) License. (h-k) Illustration of mechano-bactericidal behavior on nanoblades; the FEM result showing enhanced mechano-bactericidal stress in air flow; SEM figures of damaged *E. coli* and *S. aureus* on nanoblades. Reproduced with permission. [175] Copyright 2025, Wiley-VCH GmbH.

angles showcased physical penetration to *S. aureus*, achieving ~98 % and ~96 % inactivation rate. While regarding the top-flat nanostructure, only ~29 % of sterilization induced by bacterial deformation was observed. Furthermore, the finite element method identified a critical top conical angle of 138°, under which the induced stress (20.15 MPa) could puncture the *S. aureus* cell wall (hypothesized ultimate tensile strength = 13 MPa) (Fig. 6e-f). Based on these results, researchers proposed that the top sharpness might be paramount for bactericidal efficacy, which should be optimized primarily [173]. Nevertheless, the theoretical maximum stress required for membrane penetration still needs further verification.

Besides adjusting dimensional parameters, utilizing an extra fluid field to increase the contact stress has recently attracted extensive attention. Peng et al. first reported the hydrodynamic tearing behavior on bacteria, concluding a novel mechano-bactericidal strategy that relies on the combination of mild fluidic energy and London dispersion force between the nanotip surface and the cell membranes. The underlying mechanism of the enhanced bactericidal efficiency works as follows. When bacteria-laden water flows through the structured surfaces, bacteria collide with nanotips due to hydrodynamic forces and Brownian motion. The strong London dispersion interaction of the carbon coating transiently traps bacteria on the nanotips. Subsequent hydrodynamic drag exerts outward tension on the cell envelope at the contact area, exceeding the bacterial puncture resistance and causing mechanical tearing and cytoplasmic leakage, leading to rapid inactivation. Based on this stress-enhanced strategy, they achieved over 99.9999 % mechanical bacterial inactivation for water disinfection (*E. coli*) (Fig. 6g) [174]. Similarly, Park et al. constructed antibacterial nanoblades for bioaerosol sterilization. Under airflows (0.17–2.8 m/s), evident mechano-bactericidal efficiency promotion (Fig. 6h-k) was obtained, along with amplified stimulated Von Mises stress (0.815 MPa for *E. coli*, about 5 times higher than flat PDMS) and principal strain, exceeding critical rupture thresholds (0.56 MPa for *E. coli*). Significant bacterial cell (*E. coli* and *S. aureus*) deformation was observed on the nanostructured surface [175]. These novel enhanced strategies indicate the potential of introducing auxiliary methods into mechano-bactericidal surfaces for inactivation efficiency improvement.

Nanostructured surfaces with precise architectural configurations in contemporary biomedical engineering have been investigated for biomedical implant applications due to their inherent mechano-bactericidal properties mediated through non-chemical mechanisms. Such physical inactivation strategies effectively mitigate risks associated with antimicrobial resistance development, localized pathogen colonization, and implant-related complications [46,176–179]. Moreover, concurrently attaining high mechano-bactericidal efficiency, improved mammalian cell adhesion, and excellent biocompatibility is another research focus of implant surfaces [180]. Pham et al. first discovered the dual behavior of black silicon substrate with nanopatterns using *P. aeruginosa*, *S. aureus*, and COS-7 fibroblast cells derived from monkey kidney tissue (Fig. 6d). The assessment demonstrated that surfaces with nano-protrusions could decrease the inflammatory response and exhibit excellent biocompatibility, showing the potential for use as implantation material and mechano-bactericidal [166]. Following this conclusion, various artificial surfaces have been successfully fabricated and tested to be qualified to ensure mammalian cell adhesion [181–183]. For instance, Mo et al. constructed tiled and vertical nanoscaled lamellae (P-TL and P-VL) on a polyether-ether-ketone (PEEK) substrate. By stretching or directly penetrating, the P-TL and P-VL achieved evident mechano-bactericidal performance in stark contrast to untreated PEEK substrate. Due to the sharper edges of the nano-lamellae, more significant bacterial damage (*E. coli* and *S. aureus*) was observed on the P-VL surface. Regarding osteoblast adhesion and proliferation, however, P-TL with relatively flat topography exhibited better cell viability than P-VL, which was attributed to the sharp edges that imposed higher stress on the adhered cells, impeding their attachment and proliferation [184]. As depicted above, the sharpness of the nanostructure is a key factor in manipulating mechano-bactericidal performance. However, it might also negatively influence the mammalian cell colonization, which is important for implant surfaces. Therefore, the balance between this "surface competition" requires further systematic investigations.

4. Synergistic antibacterial surfaces based on mechano-bactericidal effect

The discussed antibacterial strategies can be categorized into two approaches: (i) anti-adhesive surfaces and (ii) mechano-bactericidal surfaces. While both exhibit effective antibacterial performance, exclusive reliance on either anti-adhesion surfaces or mechano-bactericidal surfaces presents inherent limitations in addressing severe infections, particularly over extended periods. Anti-adhesive surfaces maintain effectiveness only temporarily when intact but ultimately succumb to contamination once bacteria breach the protective layer due to absent sterilization capabilities [102,110]. Correspondingly, mechano-bactericidal surfaces inevitably accumulate dead bacteria debris, which results in potential immunological responses in addition to reducing bactericidal capacity [185,186]. Therefore, dual/multimodal function strategies emerged promptly, leveraging the synergistic work of different antibacterial capacities, including anti-adhesion and mechano-bactericidal effect to enhance the comprehensive antibacterial performance without resulting in drug resistance. The following section summarizes recent advances in innovative synergistic antibacterial strategies based on bioinspired mechano-bactericidal surfaces.

4.1. Dual functions combining anti-adhesion and mechanical penetration

Nature provides us with numerous prototypes, such as plant surfaces (lotus, pitcher plant, and other plant leaves), that employ synergistic anti-biofouling strategies, merging superwettability and mechano-bactericidal capacity to maintain a non-contaminated state. Taking advantage of air, water, or lubricant layer as a "shield", these natural surfaces coupled with high-aspect-ratio nanostructures could achieve dual-antibacterial capacities, including initial bacterial repellence and subsequent contact killing. For example, Jiang et al. revealed that the hierarchical structures composed of micro-protrusions and nanoscaled wax tubes of the lotus leaf (*Nelumbo nucifera*) (Fig. 5d) endowed the surface with anti-adhesion and contact inactivation properties. Inspired by this, they fabricated a superhydrophobic surface with hierarchical micro-/nanostructures (Fig. 7a), demonstrating exceptional non-wetting properties (WCA = 174.0°, SA < 1°) and mechano-bactericidal effect through physical penetration induced by zinc oxide nanospikes. The trapped air-layer within the dual-scale hierarchical structure after fluorination (DSF) significantly suppressed the first-stage bacteria adhesion by minimizing the interfacial contact area. Over 99 % of *E. coli* were inhibited from attachment after 24 h, while for the few adhered bacteria, over 98 % were physically killed with visible deformation, confirming the dual-antibacterial property. Moreover, the recyclability test through sterile PBS rinsing demonstrated sustained anti-adhesion and mechano-bactericidal stability, suggesting its potential as an implantable surface with synergistic antibacterial functionality [168]. Recently, Chen et al. unprecedentedly reported a similar synergistic antimicrobial effect of *Amorpha fruticosa* leaf surfaces, which combines non-wettability and mechano-bactericide induced by the randomly arranged nanoflakes (Fig. 7b). Through hydrothermal method (obtaining the copper oxide surface (COS) sample) and surface fluorination, artificial superhydrophobic surfaces with CuO nanoflakes (COSF) were fabricated, exhibiting anti-biofouling and sterilization capacity. Antibacterial tests showed 99.3 % and 99.2 % reductions in *E. coli* and *P. aeruginosa* surface coverage, respectively, along with a 99.6 % sterilization rate of *P. aeruginosa*. Such efficiency validated the role of the air cushion in suppressing bacterial adhesion, avoiding the following biofilm formation and mechano-bactericidal failure due to bacterial

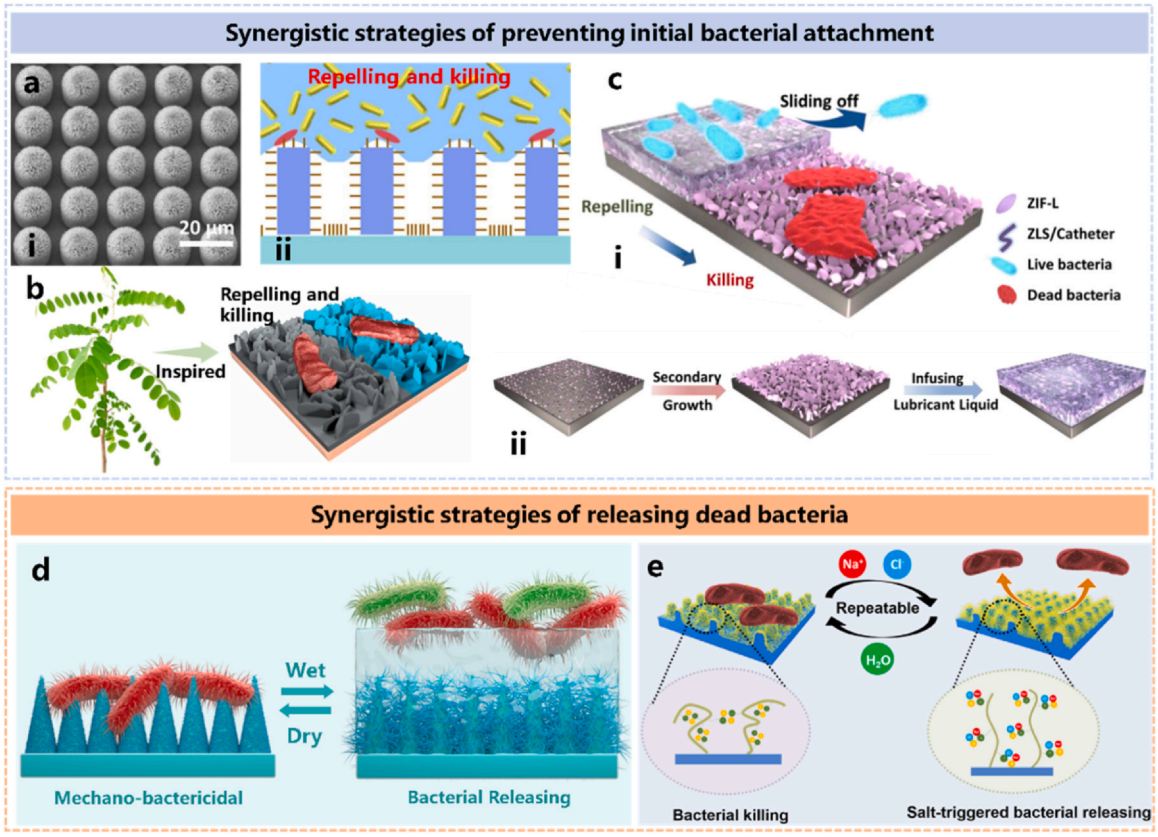

Fig. 7. Anti-adhesion/releasing synergistic surface based on mechano-bactericidal effect. (a, i) SEM figure of lotus bioinspired hierarchical superhydrophobic surface; (a, ii) the mechanism of long-term antibacterial functionality. Reproduced with permission. [168] Copyright 2020, Elsevier B.V. (b) *Amorpha fruticosa* upper leaf inspired surface with anti-adhesive and mechano-bactericidal behavior. Reproduced with permission. [187] Copyright 2023, Elsevier B.V. (c, i) Illustration of dual-functional antibacterial behavior; (c, ii) The fabrication of ZIF-L based dual-functional antibacterial surface. Reproduced with permission. [188] Copyright 2022, Elsevier Ltd. (d) Schematic of bacterial killing and releasing behavior on the PSBMA modified dragonfly inspired superhydrophilic surface. Reproduced with permission. [190] Copyright 2022, Elsevier B.V. (e) Bacterial sterilization and releasing mechanism of cicada-inspired antibacterial surface. Reproduced with permission. [191] Copyright 2022, Elsevier B.V.

intensive accumulation. Moreover, anti-abrasion evaluation proved the surface could function as a high-touched surface requiring disinfection [187]. In addition to the superhydrophobic surfaces, liquid-infused slippery surfaces with a lubricant layer could effectively inhibit bacterial contact. Taking advantage of the lubricant infusion, Hao et al. proposed a SLIPS based on oriented nanoscale zeolitic imidazolate framework-L (ZIF-L). Researchers first constructed a blade-like nanostructured surface through hydrothermal method and then embedded the lubricant into the surface, obtaining ZIF-L-based SLIPS (ZLS) (Fig. 7c). Long-term bacterial cocultivation test demonstrated that after 6 h, the control group of silicon wafer (SW) and SW with lubricant had formed irreversible biofilm, while the ZLS had no evident signal of bacterial contamination. After 12 h, the adhesion of the control group became aggravated in stark contrast to the ZLS, which remained unpolluted. Even after 48 h, ZLS invariably exhibited almost non-contaminated performance with few bacteria adhering on the surface, which could be readily washed off by water fluid. A lubricant loss simulation test was carried out to verify the purely physical sterilization, of which the blade-like structure could effectively inactivate the contact *P. aeruginosa*, indicating the dual-antibacterial ability of this SLIPS [188].

The anti-adhesion surfaces discussed earlier primarily repel initial microbial attachment, while an alternative "bacterial release" strategy addresses dead bacterial accumulation to sustain long-term functionality [189,190]. Yi et al. integrated bacterial releasing by grafting zwitterionic poly(sulfobetaine methacrylate) (PSBMA) onto ZnO nanospikes, creating a wettability-switchable surface with mechano-bactericidal effect (Fig. 7d). In dry conditions, the exposed nanospikes will physically inactivate adherent bacteria; while under hydration, the swollen polymers can release dead microbes, therefore, preserving the bactericidal efficiency. Regarding the solely mechano-bactericidal surface, long-term tests have confirmed that residual dead bacteria would gradually impair sterilization efficacy, which, as evidence, necessitates this release mechanism. The novel synergistic surface could achieve a bacterial removal efficiency of 98 % upon wetting. Over 99 % bacterial inactivation with 98 % release rates (*P. aeruginosa*) could be maintained over four cycles, demonstrating the long-term and recyclable antibacterial properties [190]. Similarly, Liu et al. developed a "killing and releasing" surface by grafting salt-responsive polyzwitterionic brushes (poly(3-(dimethyl(4-vinylbenzyl) ammonio) propyl sulfonate)) onto cicada (*Psaltoda claripennis*) wing-inspired nanopillars (Fig. 7e). Based on the reversible salt-responsive behavior of the polymeric coating, it was found that after three cycles, the switchable surface could retain a much higher bactericidal efficiency (~98.0 %) and bacterial releasing efficiency (~96.4 %), outperforming the static surfaces (77.5 % mechano-bactericidal rate, no releasing behavior). Moreover, this biomimetic surface exhibited excellent mammalian cell biocompatibility and demonstrated selective biocidal activity toward bacteria and eukaryotic cells (RBCs/L929 fibroblasts) *in vitro*. *In vivo* studies revealed a milder inflammatory response and efficient sterilization due to reduced bacterial debris accumulation, establishing a long-term reliable, AMR-free implantable platform against bacterial infections [191].

4.2. Physical strategy enhanced mechanical inactivation surfaces

Despite advancements in identifying the optimal nanostructures with maximal mechano-bactericidal efficiency [172,192–194], bacterial species with different structures present significant challenges against this strategy. Recent studies have revealed distinct mechano-bactericidal susceptibilities between Gram-negative and Gram-positive bacteria [195]. Gram-negative bacteria (e.g., *E. coli*) with thin peptidoglycan layers feature soft cell walls and low resistance to surface deformation. In contrast, Gram-positive bacteria (e.g., *S. aureus*) have multilayered peptidoglycan, which endows the bacteria with inherent rigidity and smaller bacterial deformation. Such structure distinction in structures enables the Gram-positive bacteria to resist physical stress [196,197]. Moreover, the delayed inactivation upon bacterial attachment facilitates the subsequent biofilm formation, which nanostructures struggle to eradicate. Consequently, there remains an urgent need for broad-spectrum bacterial inactivation platforms.

Fortunately, multiple physical approaches with broad-spectrum bactericidal effects have been explored to circumvent antibiotic resistance risks. Emerging as a promising physical sterilization method, photothermal therapy (PTT) (Fig. 8a) employs topical hyperthermia for microbial inactivation [198–200]. The underlying mechanism of photothermal agents (PTAs) fundamentally depends on efficiently converting near-infrared (NIR) light into topical heat, leading to cell membrane lysis and irreversible bacteria damage without causing antibiotic resistance [201,202]. Several PTAs (Fig. 8b), including carbon-based materials [203], metal-based materials [204,205], noble-metal materials [206], and polymeric materials, have been investigated [207–209]. Based on the diversified PTAs, researchers have developed photothermal inactivation surfaces, establishing this approach as an innovative solution for combating surface infections [199,210–213]. Additionally, electrostimulation offers another promising strategy, showcasing its effectiveness in bacterial integrity damage and biofilm elimination. By applying different electric field strengths, various forms of electrical stimulation can be applied to bacteria [214]. The electroporation effect, for instance, relies on strong electrical fields to break down lipid bilayers, compromise bacterial cell membranes, and cause content leakage, ultimately resulting in cell death (Fig. 8c) [215,216]. Apart from electroporation, electrocatalysis-generated hydrogen peroxide (H_2O_2) (Fig. 8d) and electro-induced intracellular reactive oxygen species (ROS) increase both have been confirmed as effective inactivation strategies [217–225]. Notably, all these inactivation strategies could be integrated into the mechano-bactericidal surfaces, promoting sterilization efficiency for both Gram-positive and Gram-negative bacteria.

Recent research has demonstrated that combining mechano-bactericidal surfaces with photothermal agents out of inorganic and organic materials can significantly enhance bacterial inactivation by generating localized heat upon near-infrared irradiation [228–230]. Meanwhile, this synergistic strategy could further lower the required irradiation power to achieve the expected sterilization efficiency by combining physical rupture, limiting the tropical hyperthermia that may result in unwanted tissue damage [231,232]. Based on the cicada wing surface, Zhang et al. designed a photothermal-therapy-enhanced mechano-antibacterial hybrid surface that exhibited remarkable broad-spectrum sterilization (Fig. 9a) and selective biocide. This environment-friendly and biocompatible photothermal coating, composed of tannic acid (TA) and ferric ion (Fe^{3+}), was fabricated through the LBL self-assembly strategy [233]. The real-time photothermal images showed the light-heat-conversion that within 1 min of NIR (808 nm) (0.6 W/cm^2) irradiation, the temperature of the surface could rapidly rise from ~17.2°C to ~57.3°C, indicating excellent hyperthermia performance. The synergistic bactericidal test of the hybrid surface against *S. aureus* and *P. aeruginosa* was evaluated. In the absence of NIR irradiation, the hybrid nanopillared surface showed a limited inactivation to bacteria, under which condition the *S. aureus* cells still had smooth membranes. While under 5 min of NIR irradiation, over 99 % Gram + and Gram- bacteria were either inviable, demonstrating the photothermal enhanced bactericidal performance. The SEM results (Fig. 9b) showed that the surface of *S. aureus* had more wrinkles and deformations with NIR

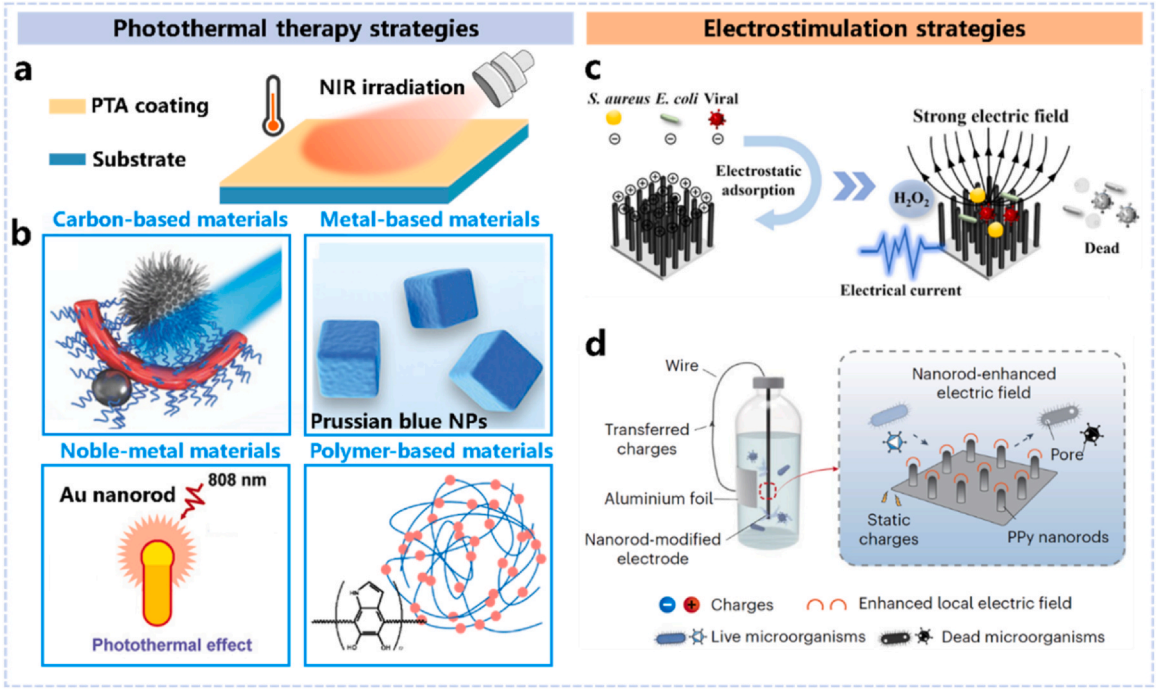

Fig. 8. Emerging physical bactericidal strategies. (a) Schematic of photothermal coated inactive surface. (b) Main categories of PTAs. Reproduced with permission. [203] Copyright 2018, John Wiley and Sons. [226] Copyright 2019, The Author(s). [227] Copyright 2021, John Wiley and Sons. (c) Synergistic inactivation of electrostimulation and electrocatalytic H_2O_2. Reproduced with permission. [218] Copyright 2024, Elsevier B.V. (d) Illustration of water disinfection system and mechanism of nanorod-enhanced electroporation effect applied on bacteria. Reproduced with permission. [219] Copyright 2024, the Author(s), under exclusive licence to Springer Nature Limited.

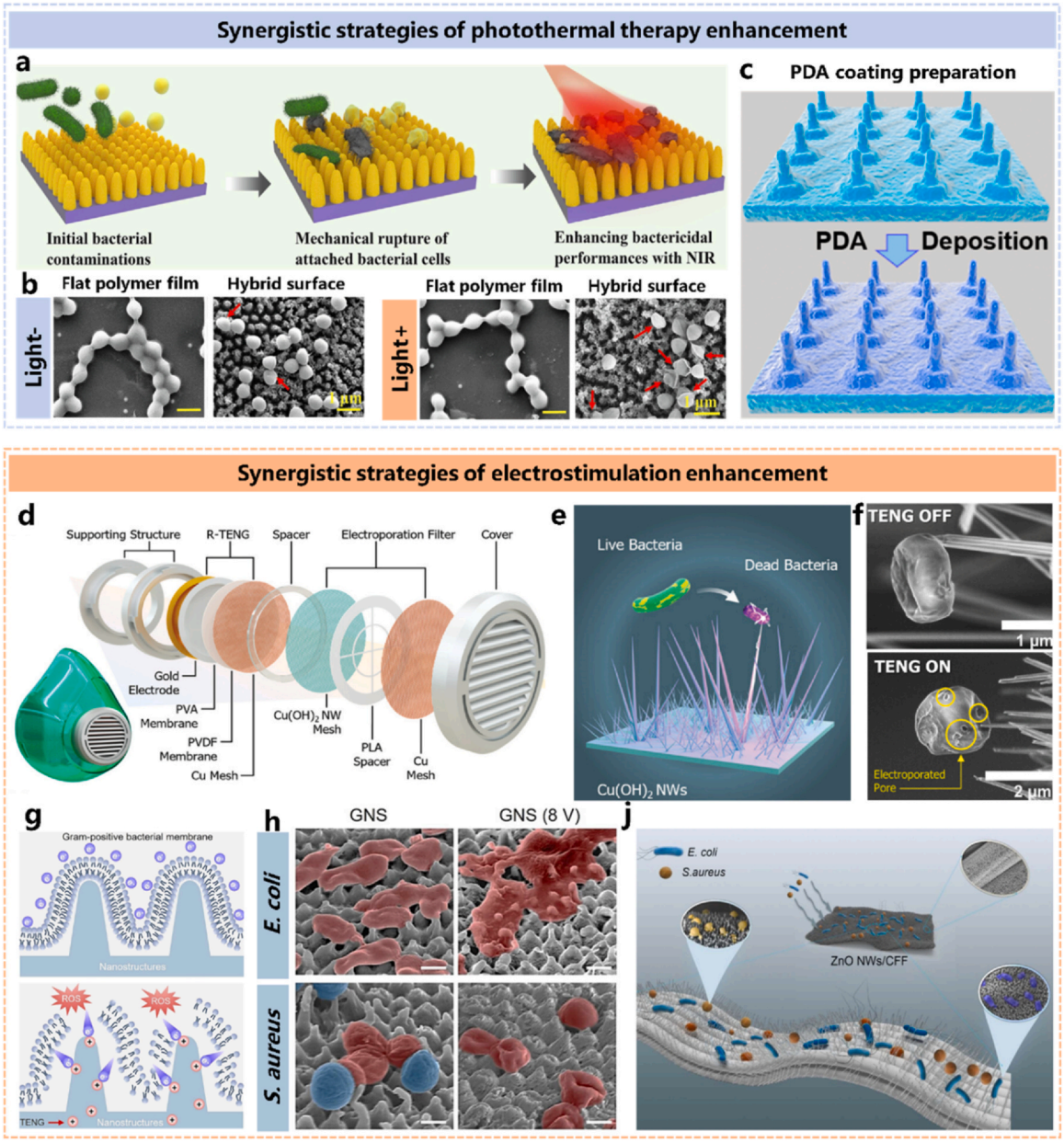

Fig. 9. Synergistic-enhanced mechano-bactericidal surfaces. (a) Schematic of synergistic bacterial inactivation based on mechano-bactericidal and photothermal effect. (b) Contrast SEM figures of *S. aureus* bacterial morphology on flat and hybrid nanopillared surfaces, with/without NIR irradiation. Reproduced with permission. [231] Copyright 2023, Elsevier Inc. (c) Illustration of PDA photothermal coating fabrication. Reproduced with permission. [228] Copyright 2023, Elsevier B.V. (d) The explosion graph of the instant disinfection mask. (e) Schematic of electroporation-enhanced antibacterial behavior on nanowires. (f) Contrast SEM figures of bacterial surface morphology with/without electroporation effect. Reproduced with permission. [236] Copyright 2024, John Wiley and Sons. (g) Illustration of enhanced mechano-bactericidal performance based on intracellular ROS increase. (h) Contrast SEM figures of bacterial surface morphology with/without electrostimulation. Reproduced with permission. [237] Copyright 2024, Elsevier Ltd. (j) The antibacterial fabrics based on synergy of piezoelectric and mechano-bactericidal effect. Reproduced with permission. [238] Copyright 2022, Elsevier Ltd.

irradiation than the lightless condition, further evidencing that the synergy of NIR light significantly amplifies the deformational effects exerted by the surface nanostructures [231]. By replacing the complex photothermal coating with PDA, Zhao et al. engineered a PTT-enhanced antibacterial surface. Cicada-wing-inspired nanopillars were obtained through the nanoimprint method, followed by the PDA deposition (Fig. 9c). The synergistic inactivation surface achieved approximately 99 % and 98 % fatality rates against *E. coli* and *S. aureus*, respectively, significantly enhancing bactericidal efficiency of nanopillared surface, particularly against *S. aureus* [228]. Another more straightforward photothermal synergy mechano-bactericidal surface was proposed by Zhang et al., based on a TiO_2 nanorod array that played a double role as mechano-stress source and photothermal agent, without introducing other chemical PTAs. The *in vitro* antibacterial test demonstrated that without NIR (808 nm), nanostructured surfaces (NS1, NS2, NS3, NS4) could only have a fatality rate of around 20 % towards *S. aureus* and *E. coli*. After 15 min of NIR (0.8 W/cm^2) irradiation, the synergistic bactericidal efficiency significantly increased to 99 %, coupled with excellent biofilm elimination. As the irradiation power added up to 1.2 W/cm^2, all the nanostructured surfaces could achieve a 100 % inactivation efficiency for both *S. aureus* and *E. coli*, indicating the success of this combined strategy [232].

Besides photothermal therapy enhancement as a synergistic bactericidal agent, electrostimulation offers another promising alternative,

enabling efficient bacterial inactivation while integrating functions, including healthcare and tissue recovery. Combining electrostimulation with bioinspired mechano-bactericidal nanostructures can demonstrate superior sterilization performance compared to single-mechanism surfaces. With external electricity, the lightning-rod effect at nanostructure tips can generate localized enhanced electric fields with high charge densities, which in turn amplify the electrostimulation effect, thereby making nanostructured surfaces an ideal platform to integrate electrostimulation [234,235]. Building upon this concept, Sim et al. proposed an electroporation-enhanced platform for respiratory protection by developing a self-powered mask consisting of a $Cu(OH)_2$-nanowires-based respiration-driven triboelectric nanogenerator (R-TENG) (Fig. 9d). A relatively high open-circuit voltage of 120 V could be generated under the regular breathing rate of an adult, successfully converting the breath energy into an amplified electrical field. While the $Cu(OH)_2$ nanowires could achieve 90 ~ 99 % *B. subtilis* sterilization through physical penetration behavior (Fig. 9e-f), the electroporation-enhanced platform further improved the inactivation efficiency to over 99.99 %. By taking advantage of the synergistic work of electrostimulation and mechano-bactericidal effect, this synergistic strategy offered an impressive instant disinfection system for respiratory healthcare [236]. Slightly different from the high voltage stimulation, Yi et al. reported a low-voltage integrated TENG consisting of gold-coated polypropylene-based bioinspired nanostructured (GNS) surfaces. By leveraging electrostimulation-enhanced intracellular ROS levels (Fig. 9g), *in vitro* studies under 8 V therapeutic triboelectric stimulation revealed a substantial enhancement in antibacterial efficacy, achieving 99.96 % against *E. coli* (compared to 83.14 % with sole nanostructure penetration) and 99.47 % against *S. aureus* (versus a 51.77 % baseline performance). SEM results showed the wrinkled bacterial morphology, further confirming the enhanced inactivation capacity, particularly for *S. aureus* (Fig. 9h). Furthermore, different nanostructured substrates, including PEEK, titanium, polycaprolactone (PCL), and PC, were used to evaluate the universally applicable properties of such synergistic strategy. It proved excellent because all of the tested substrates with various nanostructures could still exhibit over 99 % sterilization to the *S. aureus*. Additionally, the application of low voltage stimulation allows the *in vivo* biocompatibility and improvement of mammal cell proliferation and migration, due to which the patch could speed up skin wound recovery, proposing a multifunctional biomedical platform [237]. Besides relying on the TENG to provide electrostimulation, Wang et al. developed a synergistic method of piezoelectric effect, using ZnO nanowire (NW) arrays to generate interface electrons which could inhibit the bacterial growth and lead to cell death. In this research, antibacterial carbon fiber fabrics (NWs/CFF) (Fig. 9j) have been fabricated and showed an extraordinary sterilizing rate of over 99.99 % to both *S. aureus* and *E. coli,* of which 70 % of the death was accounted for the electro-effect and 30 % due to physical rupture. The same result of high fatality was obtained by testing different NW-modified fabrics, which indicated the feasibility and reliability of this electrostimulation-enhanced bactericidal surface, laying a solid fundamental for future antibacterial clothes [238].

5. Conclusions and outlook

The overuse of antibiotics has contributed to the emergence of antimicrobial resistance (AMR), accelerating the proliferation of drug-resistant bacteria. Traditional strategies based on chemical bactericidal coatings have demonstrated short-lived efficiency and many types of toxicity, including cytotoxicity, nanotoxicity, or nephrotoxicity. Inspired by the well-developed antibacterial functionality of natural prototypes, purely physical antibacterial approaches emerge as a promising alternative. In this review, antibacterial surfaces based on these bioinspired and physical approaches are delineated into two main mechanisms: bacterial repellency, leveraging different means of interfacial protective layers comprising water, gas, or lubricant, and contact-based inactivation, which harnesses physical penetration behavior of high-aspect-ratio nanostructures towards attached microorganisms. Synergistic antimicrobial platforms that properly integrate both anti-adhesion and physical bactericidal mechanisms are further discussed, with recent investigations highlighting these methods as the dominant trend that significantly promotes the antibacterial properties and effectively combats AMR.

The reproduction of naturally occurring anti-adhesion obstacle layers, including the entrapped air-layer on superhydrophobic surfaces, interlocked water/hydration layer on superhydrophilic surfaces, and the lubricant layer on SLIPS, has been achieved through surface modification. Utilizing nanofabrication techniques, micro-/nanostructured surfaces are obtained to exhibit superwettability, providing the prerequisite for repelling layer formation, which significantly inhibits bacterial attachment and subsequent biofilm formation [239]. SLIPS rely on porous or wrinkled morphology, which can lock the lubricant within them to repel bacteria [240]. Diverse strategies for constructing the anti-adhesion layer have been investigated, but their long-term stability remains a critical challenge [241,242]. Further research should prioritize the development of more efficient strategies to enhance the durability and longevity of these inhibition layers through designing novel micro-/nanostructures or utilizing self-healing strategies [243,244]. In addition to wettability, surface topography is another vital factor in influencing microbial adhesion, with its specific morphological parameters strongly linked to bacterial attachment dynamics. Micro-engineered surfaces like the shark-skin-inspired surface with microridges showcase excellent anti-adhesion properties. The mechanism behind this inhibition could be summarized as decreasing the adhesion force by minimizing the contact area between bacteria and surfaces. However, the precise influence of surface patterns and the size scale remains elusive, necessitating further systemic investigations. Moreover, irregular roughened surfaces have demonstrated the capability of modulating bacterial adhesion as well. Although the nanoscale roughness is confirmed to have excellent inhibiting capacity, there is still a lack of consensus regarding the optimal surface roughness for maximizing anti-adhesion efficacy. Novel strategies for analyzing complex interactions between different factors, such as computational simulation, are supposed to be proposed to better understand the underlying mechanism of the adhering process. Furthermore, different bacterial strains exhibit highly diverse interactions and preferences to varied surface profiles due to their divergent sizes, shapes, and surface compositions. These factors must thus be seriously considered and thoroughly evaluated while achieving optimal antibacterial efficacy in specific application scenarios. Modifications of micro-/nanostructures and geometric designs should be well customized to align with the adhesion preferences of predominant microbial species under certain circumstances, ensuring well-organized and tailored antimicrobial performance.

Mechano-bactericidal structures derived from the insect wing or plant leaf surfaces with high-aspect-ratio are well acknowledged to have an unselective physical penetration or stretching effect on bacteria [46,193,245,246]. Nanopillars, nanospikes, nanoblades, and other nanostructures can apply external stress to bacterial membranes, leading to evident bacterial cell deformation and rupture, causing non-chemical death when bacteria adhere. Being considered an effective way of pathogen sterilization, along with the ability to facilitate mammalian cell adhesion and proliferation, nanostructured surfaces are promising for catering to the requirements of implant device surfaces. Considering the differences in the composition and thickness of cell wall structures, the resistance against physical stress varies among Gram-positive bacteria like *S. aureus* and Gram-negative bacteria *E. coli*. Developing effective bactericidal nanostructures with broad-spectrum sterilization capabilities may, therefore, be a critical next step [247]. From the concept of biofilm eradication, other physical inactivation strategies, such as thermal therapy, using PTA coatings to convert light into heat to cause irreversible damage to the already-formed biofilm, have been

investigated [198,248,249]. The high efficiency of heat-converting materials is still needed. Meanwhile, biocompatibility and biodegradability are far more important. These advancements should also focus on minimizing side effects such as tissue damage and inflammation. Additionally, electro-stimulated strategies using electrical fields to apply voltage or electrocatalysis products on bacteria to achieve sterilization. TENGs and piezoelectrical materials have been involved, serving as promising methods to solve the challenge of power sources and constructing portable devices.

To address the inherent limitations of a single antibacterial strategy, synergistic physical antibacterial surfaces that are primarily based on bioinspired mechano-bactericidal nanostructures have been extensively developed. These synergistic platforms are classified according to mechanisms such as bacterial repelling/releasing with mechano-bactericidal effect or physical enhancement of mechano-bactericidal effect. Leveraging the anti-adhesion layer between the bacteria and the surface, the initial bacterial attachment will be effectively hindered, and a few “lucky” bacteria successfully adhering to the surface can be killed by the nanostructures with high-aspect-ratio. The other releasing strategies using proactive responses to sweep the dead bacteria off the surfaces can prevent the bacterial accumulation from covering the nanostructures. This repelling/releasing and killing strategy significantly prolongs the longevity of mechano-bactericidal function, preventing bacterial accumulation [250], which could decrease the penetration stress of nanostructures. Furthermore, complementary physical approaches, such as hyperthermia and electrostimulation, have displayed significant success when integrated with bactericidal nanostructures, markedly endowing controllable properties and improving broad-spectrum sterilization efficiency. By providing auxiliary stimuli, these strategies create amplified bacterial lethality, particularly Gram-positive bacteria, compared to the sole mechano-bactericidal approach. By overcoming the challenges of bacterial resistance and ensuring a broader spectrum of antimicrobial activity, this approach also expands the potential for application in diverse environments, including medical devices and surfaces prone to biofilm formation. Additionally, the combined thermal/electric stimulation could potentially reduce the reliance on chemicals, making it an environmentally friendly and sustainable solution for long-term pathogen control.

Looking ahead, the evolution and advancement of bioinspired antibacterial surfaces must address enduring challenges and capitalize on transformative opportunities alongside the rapid development and the prevailing trend of developing synergistic antimicrobial strategies, collectively paving the way for expediting the “bench to bedside” process. Firstly, achieving prolonged durability and wear-resistive robustness poses a significant hurdle for adapting physical antibacterial surfaces to clinical and nosocomial applications. Although recent investigations have integrated antifouling capabilities and enhanced antibacterial properties, current studies mainly examined the functionalities and performance over days and weeks, falling short of the clinical requirements of multitudinous scenarios such as the surface modification of chronic implants with sterilization demands over months and years. Secondly, current development and production processes for physical antibacterial surfaces, which primarily depend on techniques with precise machining and molding, are time-consuming, cost-effective, and face considerable challenges in achieving large-scale manufacturing. To bridge the gap between fabrication in research laboratories and practical deployment, innovative approaches should be further explored to promote the cost-performance ratio, the universality of substrate materials, technique accessibility, and manufacturing efficiency. Thirdly, the pursuit of biocompatibility represents a pivotal frontier: while the developed micro-/nanostructures and other physical cues effectively interrupt microbial colonization, they also significantly influence the interactions between mammalian cells and the underlying material substrates, presenting a substantial challenge to diminish the disruption to the physiological microenvironment and the surrounding tissue cells. Developing a multimodal antimicrobial platform that simultaneously inactivates bacterial attachment and mitigates tissue cell behavior such as cell migration, inflammatory response, and immunoreaction may be the optimal solution, realizing multiple bioactive functionalities involving antioxidants, anti-inflammatory effects, wound healing, immunomodulation, and angiogenesis [251–253]. Fourthly, intellectualization, controllability, and monitoring capabilities are gradually becoming paramount considerations as the emerging demands of precision medicine and personalized medication, along with the cutting-edge development of smart responsive materials, artificial intelligence, flexible electronics, machine learning, and implantable electronic devices. For example, implant materials can develop a Janus dual-function design that integrates traditional mechano-bactericidal with implantable electronics: while the outer surfaces are featured with optimum bioinspired nanostructures that are capable of eliminating a broad-spectrum of attached pathogens, the inner surfaces are equipped with strain gauges arrays to achieve strain mapping of high-sensitivity and high-resolution, enabling information acquisition of implant biomechanics for early diagnosis and prevention of catastrophic failures [254]. However, due to the limitations in electronics technology, manufacturing complexity, and cost-effectiveness, investigations into such intelligent antimicrobial designs with monitoring capacities remain limited, with considerable obstacles still to be overcome before extensive practical trials can be conducted. Additionally, widen application in different fields: not being confined to biomedical interfacial disinfection or implant surface modification, synergistic antibacterial strategies should also be improved and extended into food packaging [255], water/gas purification [256], antivirus/fungus [257,258], and other possible fields.

CRediT authorship contribution statement

Hoon Eui Jeong: Validation, Supervision, Investigation. **Rujian Jiang:** Writing – review & editing, Supervision, Resources, Funding acquisition. **Jie Zhao:** Validation, Supervision, Resources, Funding acquisition. **Luquan Ren:** Validation, Supervision, Resources. **Jiteng Zhang:** Writing – review & editing, Writing – original draft, Visualization, Validation. **Yuxiang Chen:** Writing – review & editing, Writing – original draft, Validation. **Shuo Du:** Validation, Supervision. **Mingyang Du:** Writing – review & editing, Visualization.

Declaration of Competing Interest

The authors declare that they have no known competing financial interests or personal relationships that could have appeared to influence the work reported in this paper.

Acknowledgements

The authors gratefully acknowledge the financial support through the National Science Foundation of China (No. 52305317); the research collaboration project between the National Natural Science Foundation of China and the National Research Foundation of Korea (No. W2412095), Natural Science Foundation of Shandong Province (No. ZR2022QB040, ZR2022QH006, ZR20230B113), and the Youth Innovation Team of Shandong Province (2024KJH045).

References

[1] P. Dadgostar, Antimicrobial resistance: implications and costs, Infect. Drug Resist 12 (2019) 3903–3910.
[2] T.J. Hall, V.M. Villapun, O. Addison, et al., A call for action to the biomaterial community to tackle antimicrobial resistance, Biomater. Sci. 8 (18) (2020) 4951–4974.
[3] A. Lakhani, K. Jindal, K. Khatri, Antimicrobial resistance (AMR) in orthopaedic surgeries: a complex issue and global threat, J. Orthop. Rep. 4 (4) (2025) 100466.
[4] K.W.K. Tang, B.C. Millar, J.E. Moore, Antimicrobial resistance (AMR), Br. J. Biomed. Sci. 80 (2023) 11387.

[5] A.D. Pye, D.E. Lockhart, M.P. Dawson, et al., A review of dental implants and infection, J. Hosp. Infect. 72 (2) (2009) 104–110.
[6] P.J. Sanderson, Infection in orthopaedic implants, J. Hosp. Infect. 18 (1991) 367–375.
[7] G. Gebreyohannes, A. Nyerere, C. Bii, et al., Challenges of intervention, treatment, and antibiotic resistance of biofilm-forming microorganisms, Heliyon 5 (8) (2019) e02192.
[8] P. Shree, C.K. Singh, K.K. Sodhi, et al., Biofilms: understanding the structure and contribution towards bacterial resistance in antibiotics, Med. Micro 16 (2023) 100084.
[9] C. Michaelis, E. Grohmann, Horizontal gene transfer of antibiotic resistance genes in biofilms, Antibiotic 12 (2) (2023) 328.
[10] V.A. Baulin, D.P. Linklater, S. Juodkazis, et al., Exploring broad-spectrum antimicrobial nanotopographies: implications for bactericidal, antifungal, and virucidal surface design, ACS Nano 19 (13) (2025) 12606–12625.
[11] G. O'Toole, H.B. Kaplan, R. Kolter, Biofilm formation as microbial development, Annu. Rev. Microbiol 54 (2000) 49–79.
[12] X. Wang, M. Liu, C. Yu, et al., Biofilm formation: mechanistic insights and therapeutic targets, Mol. Biomed. 4 (1) (2023) 49.
[13] K. Sauer, P. Stoodley, D.M. Goeres, et al., The biofilm life cycle: expanding the conceptual model of biofilm formation, Nat. Rev. Microbiol 20 (10) (2022) 608–620.
[14] S. Singh, S. Datta, K.B. Narayanan, et al., Bacterial exo-polysaccharides in biofilms: Role in antimicrobial resistance and treatments, J. Genet. Eng. Biotechnol. 19 (1) (2021) 140.
[15] D. Pavithra, M. Doble, Biofilm formation, bacterial adhesion and host response on polymeric implants–issues and prevention, Biomed. Mater. 3 (3) (2008) 034003.
[16] P. Li, R. Yin, J. Cheng, et al., Bacterial biofilm formation on biomaterials and approaches to its treatment and prevention, Int. J. Mol. Sci. 24 (14) (2023).
[17] F. Ghilini, D.E. Pissinis, A. Minan, et al., How functionalized surfaces can inhibit bacterial adhesion and viability, ACS Biomater. Sci. Eng. 5 (10) (2019) 4920–4936.
[18] P.S. Brunetto, K.M. Fromm, Antimicrobial coatings for implant surfaces, Chimia 62 (4) (2008).
[19] L. Zhao, P.K. Chu, Y. Zhang, et al., Antibacterial coatings on titanium implants, J. Biomed. Mater. Res. B Appl. Biomater. 91 (1) (2009) 470–480.
[20] N. Gugala, J.A. Lemire, R.J. Turner, The efficacy of different anti-microbial metals at preventing the formation of, and eradicating bacterial biofilms of pathogenic indicator strains, J. Antibiot. 70 (6) (2017) 775–780.
[21] M. Cloutier, D. Mantovani, F. Rosei, Antibacterial coatings: challenges, perspectives, and opportunities, Trends Biotechnol. 33 (11) (2015) 637–652.
[22] L.Q. Chen, L. Fang, J. Ling, et al., Nanotoxicity of silver nanoparticles to red blood cells: size dependent adsorption, uptake, and hemolytic activity, Chem. Res. Toxicol. 28 (3) (2015) 501–509.
[23] A. Gallardo-Godoy, C. Muldoon, B. Becker, et al., Activity and predicted nephrotoxicity of synthetic antibiotics based on polymyxin b, J. Med. Chem. 59 (3) (2016) 1068–1077.
[24] S. Lakhundi, K. Zhang, Methicillin-resistant Staphylococcus aureus: molecular characterization, evolution, and epidemiology, Clin. Microbiol. Rev. 31 (4) (2018) 10–1128.
[25] C.J. Murray, K.S. Ikuta, F. Sharara, et al., Global burden of bacterial antimicrobial resistance in 2019: a systematic analysis, Lancet 399 (10325) (2022) 629–655.
[26] A. Jaggessar, H. Shahali, A. Mathew, et al., Bio-mimicking nano and microstructured surface fabrication for antibacterial properties in medical implants, J. Nanobiotechnol 15 (1) (2017).
[27] A. Tripathy, P. Sen, B. Su, et al., Natural and bioinspired nanostructured bactericidal surfaces, Adv. Colloid Interface Sci. 248 (2017) 85–104.
[28] J.B. Yang, H. Lee, D.R. Kim, Design and fabrication of nature-inspired surfaces for anti-fouling: a review, Int. J. Precis. Eng. Manuf. Green. Technol. 12 (1) (2024) 321–347.
[29] Y. Wu, P. Liu, B. Mehrjou, et al., Interdisciplinary-inspired smart antibacterial materials and their biomedical applications, Adv. Mater. 36 (17) (2024) e2305940.
[30] M.I. Kayes, A.J. Galante, N.A. Stella, et al., Stable lotus leaf-inspired hierarchical, fluorinated polypropylene surfaces for reduced bacterial adhesion, React. Funct. Polym. 128 (2018) 40–46.
[31] J. Li, B. Lu, Z. Cheng, et al., Designs and recent progress of “pitcher plant effect” inspired ultra-slippery surfaces: a review, Prog. Org. Coat. 191 (2024) 108460.
[32] Y. Peng, G. Wen, X. Gou, et al., Bioinspired fish-scale-like stainless steel surfaces with robust underwater anti-crude-oil-fouling and self-cleaning properties, Sep. Purif. Technol. 202 (2018) 111–118.
[33] Y. Chen, J. Ao, J. Zhang, et al., Bioinspired superhydrophobic surfaces, inhibiting or promoting microbial contamination? Mater. Today 67 (2023) 468–494.
[34] A.K. Epstein, T.S. Wong, R.A. Belisle, et al., Liquid-infused structured surfaces with exceptional anti-biofouling performance, Proc. Natl. Acad. Sci. 109 (33) (2012) 13182–13187.
[35] Z. Li, Z. Guo, Bioinspired surfaces with wettability for antifouling application, Nanoscale 11 (47) (2019) 22636–22663.
[36] M.J. Mayser, H.F. Bohn, M. Reker, et al., Measuring air layer volumes retained by submerged floating-ferns salvinia and biomimetic superhydrophobic surfaces, Beilstein J. Nanotechnol. 5 (2014) 812–821.
[37] G.D. Bixler, B. Bhushan, Bioinspired rice leaf and butterfly wing surface structures combining shark skin and lotus effects, Soft Matter 8 (44) (2012).
[38] H. Chen, P. Zhang, L. Zhang, et al., Continuous directional water transport on the peristome surface of Nepenthes alata, Nature 532 (7597) (2016) 85–89.
[39] W. Barthlott, Christoph Neinhuis, Purity of the sacred lotus, or escape from contamination in biological surfaces, Planta 202 (1) (1997) 1–8.
[40] P. Zhang, L. Lin, D. Zang, et al., Designing bioinspired anti-biofouling surfaces based on a superwettability strategy, Small 13 (4) (2017) 1503334.
[41] G.D. Bixler, A. Theiss, B. Bhushan, et al., Anti-fouling properties of microstructured surfaces bio-inspired by rice leaves and butterfly wings, J. Colloid Interface Sci. 419 (2014) 114–133.
[42] M. Liu, S. Wang, Z. Wei, et al., Bioinspired design of a superoleophobic and low adhesive water/solid interface, Adv. Mater. 21 (6) (2009) 665–669.
[43] D. Rana, T. Matsuura, Surface modifications for antifouling membranes, Chem. Rev. 110 (4) (2010) 2448–2471.
[44] G.D. Kang, Y.M. Cao, Development of antifouling reverse osmosis membranes for water treatment: a review, Water Res 46 (3) (2012) 584–600.
[45] D.P. Linklater, S. Juodkazis, E.P. Ivanova, Nanofabrication of mechano-bactericidal surfaces, Nanoscale 9 (43) (2017) 16564–16585.
[46] D.P. Linklater, V.A. Baulin, S. Juodkazis, et al., Mechano-bactericidal actions of nanostructured surfaces, Nat. Rev. Microbiol 19 (1) (2021) 8–22.
[47] C.D. Bandara, S. Singh, I.O. Afara, et al., Bactericidal effects of natural nanotopography of dragonfly wing on Escherichia coli, ACS Appl. Mater. Interfaces 9 (8) (2017) 6746–6760.
[48] J. Jenkins, J. Mantell, C. Neal, et al., Antibacterial effects of nanopillar surfaces are mediated by cell impedance, penetration and induction of oxidative stress, Nat. Commun. 11 (1) (2020) 1626.
[49] C.R. Arciola, D. Campoccia, L. Montanaro, Implant infections: adhesion, biofilm formation and immune evasion, Nat. Rev. Microbiol 16 (7) (2018) 397–409.
[50] J.M. Schierholz, J. Beuth, Implant infections: a haven for opportunistic bacteria, J. Hosp. Infect. 49 (2) (2001) 87–93.
[51] W.M. Dunne Jr., Bacterial adhesion: seen any good biofilms lately? Clin. Microbiol. Rev. 15 (2) (2002) 155–166.
[52] L.S.C. Crouzet M, V.S. Brözel, et al., Exploring early steps in biofilm formation set-up of an experimental system for molecular studies, BMC Microbiol 14 (2014) 1–12.
[53] T. Kilic, E.B. Bali, Biofilm control strategies in the light of biofilm-forming microorganisms, World J. Microbiol. Biotechnol. 39 (5) (2023) 131.
[54] S.A. Aransiola, B. Selvaraj, N.R. Maddela, Bacterial biofilm formation and antibiofilm strategies, Res. Microbiol 175 (3) (2024) 104172.
[55] M. Zhang, S. Feng, L. Wang, et al., Lotus effect in wetting and self-cleaning, Biotribology 5 (2016) 31–43.
[56] T. Darmanin, F. Guittard, Superhydrophobic and superoleophobic properties in nature, Mater. Today 18 (5) (2015) 273–285.
[57] K. Yang, J. Shi, L. Wang, et al., Bacterial anti-adhesion surface design: Surface patterning, roughness and wettability: a review, J. Mater. Sci. Technol. 99 (2022) 82–100.
[58] J. Drelich, E. Chibowski, Superhydrophilic and superwetting surfaces: definition and mechanisms of control, Langmuir 26 (24) (2010) 18621–18623.
[59] J. Jeevahan, M. Chandrasekaran, G. Britto Joseph, et al., Superhydrophobic surfaces: a review on fundamentals, applications, and challenges, J. Coat. Technol. Res. 15 (2) (2018) 231–250.
[60] M.S. Lee, H.R. Hussein, S.W. Chang, et al., Nature-inspired surface structures design for antimicrobial applications, Int. J. Mol. Sci. 24 (2) (2023) 1348.
[61] Y.L. Zhan, M. Ruan, W. Li, et al., Fabrication of anisotropic PTFE superhydrophobic surfaces using laser microprocessing and their self-cleaning and anti-icing behavior, Colloids Surf. A 535 (2017) 8–15.
[62] H.-X. Huang, X. Wang, Biomimetic fabrication of micro-/nanostructure on polypropylene surfaces with high dynamic superhydrophobic stability, Mater. Today Commun. 19 (2019) 487–494.
[63] A. Chen, S. Ding, J. Huang, et al., Fabrication of superrepellent microstructured polypropylene/graphene surfaces with enhanced wear resistance, J. Mater. Sci. 54 (5) (2018) 3914–3926.
[64] D.A.S. Cortese B, M. Manca, et al., Superhydrophobicity due to the hierarchical scale roughness of PDMS surfaces, Langmuir 24 (6) (2008) 2712–2718.
[65] S. Sohrabi, H. Pazokian, B. Ghafary, et al., Superhydrophobic-antibacterial polycarbonate fabrication using excimer laser treatment, Optik 262 (2022).
[66] A.Y.Y. Ho, E. Luong Van, C.T. Lim, et al., Lotus bioinspired superhydrophobic, self-cleaning surfaces from hierarchically assembled templates, J. Polym. Sci. Part B Polym. Phys. 52 (8) (2014) 603–609.
[67] J. Liang, K. Liu, D. Wang, et al., Facile fabrication of superhydrophilic/superhydrophobic surface on titanium substrate by single-step anodization and fluorination, Appl. Surf. Sci. 338 (2015) 126–136.
[68] X. Zhang, Y. Wan, B. Ren, et al., Preparation of superhydrophobic surface on titanium alloy via micro-milling, anodic oxidation and fluorination, Micromachines 11 (3) (2020).
[69] Z. Wang, B. Ren, Preparation of superhydrophobic titanium surface via the combined modification of hierarchical micro/nanopatterning and fluorination, J. Coat. Technol. Res. 19 (3) (2022) 967–975.
[70] S. Parvate, P. Dixit, S. Chattopadhyay, Superhydrophobic surfaces: insights from theory and experiment, J. Phys. Chem. B 124 (8) (2020) 1323–1360.
[71] Q. Pan, Y. Cao, W. Xue, et al., Picosecond laser-textured stainless steel superhydrophobic surface with an antibacterial adhesion property, Langmuir 35 (35) (2019) 11414–11421.
[72] S.S. Ray, Y.I. Park, H. Park, et al., Surface innovation to enhance anti-droplet and hydrophobic behavior of breathable compressed-polyurethane masks, Environ. Technol. Innov. 20 (2020) 101093.
[73] H. Zhong, Z. Zhu, J. Lin, et al., Reusable and recyclable graphene masks with outstanding superhydrophobic and photothermal performances, ACS Nano 14 (5) (2020) 6213–6221.
[74] R. Soni, S.R. Joshi, M. Karmacharya, et al., Superhydrophobic and self-sterilizing surgical masks spray-coated with carbon nanotubes, ACS Appl. Nano Mater. 4 (8) (2021) 8491–8499.

[75] H. Zhong, Z. Zhu, P. You, et al., Plasmonic and superhydrophobic self-decontaminating n95 respirators, ACS Nano 14 (7) (2020) 8846–8854.
[76] M. Laad, B. Ghule, Fabrication techniques of superhydrophobic coatings: a comprehensive review, Phys. Status Solidi (a) 219 (16) (2022) 2200109.
[77] K. Li, J. Lei, Y. Xie, et al., An easy-to-implement method for fabricating superhydrophobic surfaces inspired by taro leaf, Sci. China Technol. Sci. 64 (12) (2021) 2676–2687.
[78] Z. Chen, L. Hao, A. Chen, et al., A rapid one-step process for fabrication of superhydrophobic surface by electrodeposition method, Electrochim. Acta 59 (2012) 168–171.
[79] M. Ye, Z. Tian, S. Wang, et al., Simple preparation of environmentally friendly and durable superhydrophobic antibacterial paper, Cellulose 30 (4) (2022) 2427–2440.
[80] E. Nyankson, H. Agbe, G.K.S. Takyi, et al., Recent advances in nanostructured superhydrophobic surfaces: fabrication and long-term durability challenges, Curr. Opin. Chem. Eng. 36 (2022).
[81] T. Wang, L. Huang, Y. Liu, et al., Robust biomimetic hierarchical diamond architecture with a self-cleaning, antibacterial, and antibiofouling surface, ACS Appl. Mater. Interfaces 12 (21) (2020) 24432–24441.
[82] D. Wang, Q. Sun, M.J. Hokkanen, et al., Design of robust superhydrophobic surfaces, Nature 582 (7810) (2020) 55–59.
[83] S. Zhao, X. Yang, Y. Xu, et al., A sprayable superhydrophobic dental protectant with photo-responsive anti-bacterial, acid-resistant, and anti-fouling functions, Nano Res. 15 (6) (2022) 5245–5255.
[84] X. Zang, J. Bian, Y. Ni, et al., A robust biomimetic superhydrophobic coating with superior mechanical durability and chemical stability for inner pipeline protection, Adv. Sci. 11 (12) (2024) e2305839.
[85] T. Verho, C. Bower, P. Andrew, et al., Mechanically durable superhydrophobic surfaces, Adv. Mater. 23 (5) (2011) 673–678.
[86] J. Groten, J. Ruhe, Surfaces with combined microscale and nanoscale structures: a route to mechanically stable superhydrophobic surfaces? Langmuir 29 (11) (2013) 3765–3772.
[87] Y. Qing, S. Shi, C. Lv, et al., Microskeleton-nanofiller composite with mechanical super-robust superhydrophobicity against abrasion and impact, Adv. Func. Mater. 30 (39) (2020).
[88] S. Haghanifar, A.J. Galante, M. Zarei, et al., Mechanically durable, super-repellent 3D printed microcell/nanoparticle surfaces, Nano Res. 15 (6) (2022) 5678–5686.
[89] T. Huhtamaki, X. Tian, J.T. Korhonen, et al., Surface-wetting characterization using contact-angle measurements, Nat. Protoc. 13 (7) (2018) 1521–1538.
[90] S. Chen, L. Li, C. Zhao, et al., Surface hydration: principles and applications toward low-fouling/nonfouling biomaterials, Polymer 51 (23) (2010) 5283–5293.
[91] J. Drelich, E. Chibowski, D.D. Meng, et al., Hydrophilic and superhydrophilic surfaces and materials, Softw. Matter 7 (21) (2011) 9804.
[92] M. d P. Madeira, S.B.S. Gusmão, I.S. de Lima, et al., Deposition of sodium titanate nanotubes: superhydrophilic, Surf. Antibact. Approach J. Mater. Res. Technol. 19 (2022) 2104–2114.
[93] H. Younas, Y. Fei, J. Shao, et al., Developing an antibacterial super-hydrophilic barrier between bacteria and membranes to mitigate the severe impacts of biofouling, Biofouling 32 (9) (2016) 1089–1102.
[94] S. Park, H.H. Kim, S.B. Yang, et al., A polysaccharide-based antibacterial coating with improved durability for clear overlay appliances, ACS Appl. Mater. Interfaces 10 (21) (2018) 17714–17721.
[95] J. Yang, H. Song, X. Yan, et al., Superhydrophilic and superoleophobic chitosan-based nanocomposite coatings for oil/water separation, Cellulose 21 (3) (2014) 1851–1857.
[96] J. Yang, L. Lin, Q. Wang, et al., Engineering a superwetting membrane with spider-web structured carboxymethyl cellulose gel layer for efficient oil-water separation based on biomimetic concept, Int. J. Biol. Macromol. 222 (Pt B) (2022) 2603–2614.
[97] B.P. Tripathi, N.C. Dubey, M. Stamm, Polyethylene glycol cross-linked sulfonated polyethersulfone based filtration membranes with improved antifouling tendency, J. Membr. Sci. 453 (2014) 263–274.
[98] P. Wang, Y.-L. Zhang, K.-L. Fu, et al., Zinc-coordinated polydopamine surface with a nanostructure and superhydrophilicity for antibiofouling and antibacterial applications, Mater. Adv. 3 (13) (2022) 5476–5487.
[99] X. Lin, M. Yang, H. Jeong, et al., Durable superhydrophilic coatings formed for anti-biofouling and oil–water separation, J. Membr. Sci. 506 (2016) 22–30.
[100] X.-D. Weng, Y.-L. Ji, R. Ma, et al., Superhydrophilic and antibacterial zwitterionic polyamide nanofiltration membranes for antibiotics separation, J. Membr. Sci. 510 (2016) 122–130.
[101] C. Wen, H. Guo, J. Yang, et al., Zwitterionic hydrogel coated superhydrophilic hierarchical antifouling floater enables unimpeded interfacial steam generation and multi-contamination resistance in complex conditions, Chem. Eng. J. 421 (2021) 130344.
[102] H. Zhang, F. Wang, Z. Guo, The antifouling mechanism and application of bio-inspired superwetting surfaces with effective antifouling performance, Adv. Colloid Interface Sci. 325 (2024).
[103] Z. Huang, H. Ghasemi, Hydrophilic polymer-based anti-biofouling coatings: preparation, mechanism, and durability, Adv. Colloid Interface Sci. 284 (2020) 102264.
[104] L. Li, B. Yan, L. Zhang, et al., Mussel-inspired antifouling coatings bearing polymer loops, Chem. Commun. 51 (87) (2015) 15780–15783.
[105] B. Li, P. Jain, J. Ma, et al., Trimethylamine n-oxide-derived zwitterionic polymers: a new class of ultralow fouling bioinspired materials, Sci. Adv. 5 (6) (2019) eaaw9562.
[106] Q. Shao, Y. He, A.D. White, et al., Difference in hydration between carboxybetaine and sulfobetaine, J. Phys. Chem. B 114 (49) (2010) 16625–16631.
[107] Y. Ke, H. Meng, Z. Du, et al., Bioinspired super-hydrophilic zwitterionic polymer armor combats thrombosis and infection of vascular catheters, Bioact. Mater. 37 (2024) 493–504.
[108] L. Gao, X. Liu, M. Xu, et al., Biodegradable anti-biofilm fiber-membrane ureteral stent constructed with a robust biomimetic superhydrophilic polycationic hydration surface exhibiting synergetic antibacterial and antiprotein properties, Small 17 (20) (2021) e2006815.
[109] S. Park, J. Park, J. Heo, et al., Polysaccharide-based superhydrophilic coatings with antibacterial and anti-inflammatory agent-delivering capabilities for ophthalmic applications, J. Ind. Eng. Chem. 68 (2018) 229–237.
[110] G.B. Hwang, K. Page, A. Patir, et al., The anti-biofouling properties of superhydrophobic surfaces are short-lived, ACS Nano 12 (6) (2018) 6050–6058.
[111] T. Chen, J. Pang, X. Liu, et al., Anti-biofilm super-hydrophilic gel sensor for saliva glucose monitoring, Nano Today 55 (2024).
[112] H.F. Bohn, W. Federle, Insect aquaplaning: nepenthes pitcher plants capture prey with the peristome, a fully wettable water-lubricated anisotropic surface, Proc. Natl. Acad. Sci. 101 (39) (2004) 14138–14143.
[113] T.-S. Wong, S.H. Kang, S.K.Y. Tang, et al., Bioinspired self-repairing slippery surfaces with pressure-stable omniphobicity, Nature 477 (7365) (2011) 443–447.
[114] J. Li, E. Ueda, D. Paulssen, et al., Slippery lubricant-infused surfaces: properties and emerging applications, Adv. Funct. Mater. 29 (4) (2018) 1802317.
[115] M. Villegas, Y. Zhang, N. Abu Jarad, et al., Liquid-infused surfaces: a review of theory, design, and applications, ACS Nano 13 (8) (2019) 8517–8536.
[116] S. Sunny, G. Cheng, D. Daniel, et al., Transparent antifouling material for improved operative field visibility in endoscopy, Proc. Natl. Acad. Sci. 113 (42) (2016) 11676–11681.
[117] D.C. Leslie, A. Waterhouse, J.B. Berthet, et al., A bioinspired omniphobic surface coating on medical devices prevents thrombosis and biofouling, Nat. Biotechnol. 32 (11) (2014) 1134–1140.
[118] M. Xu, Z. Xu, Z. Jiang, et al., Biomimicking integrates peristome surface of Nepenthes alata onto biliary stents tips, Chem. Eng. J. 454 (2023) 140064.
[119] D. Tripathi, P. Ray, A.V. Singh, et al., Durability of slippery liquid-infused surfaces: challenges and advances, Coatings 13 (6) (2023).
[120] P. Kim, M.J. Kreder, J. Alvarenga, et al., Hierarchical or not? Effect of the length scale and hierarchy of the surface roughness on omniphobicity of lubricant-infused substrates, Nano Lett. 13 (4) (2013) 1793–1799.
[121] S. Jiao, D. Ma, Z. Cheng, et al., Super-slippery poly(dimethylsiloxane) brush surfaces: from fabrication to practical application, Chempluschem 88 (1) (2023) e202200379.
[122] S. Lv, X. Yang, Q. Liu, et al., Solid-like slippery surface with excellent comprehensive performance, Langmuir 39 (31) (2023) 11073–11080.
[123] H.H. Tran, Y. Kim, C. Ternon, et al., Lubricant depletion-resistant slippery liquid-infused porous surfaces via capillary rise lubrication of nanowire array, Adv. Mater. Interfaces 8 (7) (2021).
[124] B. Li, K. Huang, S. Xue, et al., Robust slippery liquid-infused porous surfaces with fast self-replenishment properties for anticontaminant, anti-icing, and anticorrosion applications on magnesium alloys, ACS Appl. Mater. Interfaces 17 (12) (2025) 19105–19116.
[125] F.W. Wang, J. Sun, A. Tuteja, Material design for durable lubricant-infused surfaces that can reduce liquid and solid fouling, ACS Nano 19 (19) (2025) 18075–18094.
[126] L. Chen, S. Huang, R.H.A. Ras, et al., Omniphobic liquid-like surfaces, Nat. Rev. Chem. 7 (2) (2023) 123–137.
[127] Z. Zhang, Y. Bai, R. Han, et al., Improving antifouling functions of titanium alloys by robust slippery liquid-infused porous surfaces with tailored multiscale structures, Chem. Eng. J. 478 (2023) 147342.
[128] R.J. Crawford, H.K. Webb, V.K. Truong, et al., Surface topographical factors influencing bacterial attachment, Adv. Colloid Interface Sci. 179-182 (2012) 142–149.
[129] K.K. Chung, J.F. Schumacher, E.M. Sampson, et al., Impact of engineered surface microtopography on biofilm formation of Staphylococcus aureus, Biointerphases 2 (2) (2007) 89–94.
[130] N. Epperlein, F. Menzel, K. Schwibbert, et al., Influence of femtosecond laser produced nanostructures on biofilm growth on steel, Appl. Surf. Sci. 418 (2017) 420–424.
[131] P. Halder, M. Nasabi, N. Jayasuriya, et al., An assessment of the dynamic stability of microorganisms on patterned surfaces in relation to biofouling control, Biofouling 30 (6) (2014) 695–707.
[132] M.V. Graham, A.P. Mosier, T.R. Kiehl, et al., Development of antifouling surfaces to reduce bacterial attachment, Softw. Matter 9 (27) (2013) 6235.
[133] M. Palacios-Cuesta, A.L. Cortajarena, O. García, et al., Patterning of individual Staphylococcus aureus bacteria onto photogenerated polymeric surface structures, Polym. Chem. 6 (14) (2015) 2677–2684.
[134] Y. Wang, J.F. da Silva Domingues, G. Subbiahdoss, et al., Conditions of lateral surface confinement that promote tissue-cell integration and inhibit biofilm growth, Biomaterials 35 (21) (2014) 5446–5452.
[135] E. Fadeeva, V.K. Truong, M. Stiesch, et al., Bacterial retention on superhydrophobic titanium surfaces fabricated by femtosecond laser ablation, Langmuir 27 (6) (2011) 3012–3019.
[136] M. Yang, Y. Ding, X. Ge, et al., Control of bacterial adhesion and growth on honeycomb-like patterned surfaces, Colloids Surf. B Biointerfaces 135 (2015) 549–555.
[137] S. Wu, B. Zhang, Y. Liu, et al., Influence of surface topography on bacterial adhesion: a review (review), Biointerphases 13 (6) (2018).
[138] H. Jin, L. Tian, W. Bing, et al., Bioinspired marine antifouling coatings: status, prospects, and future, Prog. Mater. Sci. 124 (2022) 100889.

[139] S.W. Lee, K.S. Phillips, H. Gu, et al., How microbes read the map: effects of implant topography on bacterial adhesion and biofilm formation, Biomaterials 268 (2021) 120595.
[140] H. Gu, K.W. Kolewe, D. Ren, Conjugation in Escherichia coli biofilms on poly (dimethylsiloxane) surfaces with microtopographic patterns, Langmuir 33 (12) (2017) 3142–3150.
[141] M. Prudhomme, L. Attaiech, G. Sanchez, et al., Antibiotic stress induces genetic transformability in the human pathogen Streptococcus pneumoniae, Science 313 (5783) (2006) 89–92.
[142] M. Mu, S. Liu, W. DeFlorio, et al., Influence of surface roughness, nanostructure, and wetting on bacterial adhesion, Langmuir 39 (15) (2023) 5426–5439.
[143] K. Manabe, S. Nishizawa, S. Shiratori, Porous surface structure fabricated by breath figures that suppresses Pseudomonas aeruginosa biofilm formation, ACS Appl. Mater. Interfaces 5 (22) (2013) 11900–11905.
[144] R. Helbig, D. Günther, J. Friedrichs, et al., The impact of structure dimensions on initial bacterial adhesion, Biomater. Sci. 4 (7) (2016) 1074–1078.
[145] A. Lu, Y. Gao, T. Jin, et al., Effects of surface roughness and texture on the bacterial adhesion on the bearing surface of bio-ceramic joint implants: an in vitro study, Ceram. Int. 46 (5) (2020) 6550–6559.
[146] T. Wassmann, S. Kreis, M. Behr, et al., The influence of surface texture and wettability on initial bacterial adhesion on titanium and zirconium oxide dental implants, Int. J. Implant Dent. 3 (1) (2017) 32.
[147] C. Meel, N. Kouzel, E.R. Oldewurtel, et al., Three-dimensional obstacles for bacterial surface motility, Small 8 (4) (2012) 530–534.
[148] Y.-R. Chang, E.R. Weeks, W.A. Ducker, Surface topography hinders bacterial surface motility, ACS Appl. Mater. Interfaces 10 (11) (2018) 9225–9234.
[149] N. Lu, W. Zhang, Y. Weng, et al., Fabrication of PDMS surfaces with micro patterns and the effect of pattern sizes on bacteria adhesion, Food Control 68 (2016) 344–351.
[150] N. Thewes, A. Thewes, P. Loskill, et al., Stochastic binding of Staphylococcus aureus to hydrophobic surfaces, Softw. Matter 11 (46) (2015) 8913–8919.
[151] C. Lüdecke, J. Bossert, M. Roth, et al., Physical vapor deposited titanium thin films for biomedical applications: reproducibility of nanoscale surface roughness and microbial adhesion properties, Appl. Surf. Sci. 280 (2013) 578–589.
[152] C. Spengler, F. Nolle, J. Mischo, et al., Strength of bacterial adhesion on nanostructured surfaces quantified by substrate morphometry, Nanoscale 11 (42) (2019) 19713–19722.
[153] N. Mitik-Dineva, J. Wang, V.K. Truong, et al., Escherichia coli, Pseudomonas aeruginosa, and Staphylococcus aureus attachment patterns on glass surfaces with nanoscale roughness, Curr. Microbiol 58 (3) (2008) 268–273.
[154] K. Azelmad, F. Hamadi, R. Mimouni, et al., Adhesion of Staphylococcus aureus and Staphylococcus xylosus to materials commonly found in catering and domestic kitchens, Food Control 73 (2017) 156–163.
[155] A.Z. Komaromy, S. Li, H. Zhang, et al., Arrays of nano-structured surfaces to probe the adhesion and viability of bacteria, Microelectron. Eng. 91 (2012) 39–43.
[156] K.A. Whitehead, D. Rogers, J. Colligon, et al., Use of the atomic force microscope to determine the effect of substratum surface topography on the ease of bacterial removal, Colloids Surf. B 51 (1) (2006) 44–53.
[157] A. Miñán, P.L. Schilardi, M. Fernández Lorenzo de Mele, The importance of 2d aggregates on the antimicrobial resistance of Staphylococcus aureus sessile bacteria (C), Mater. Sci. Eng. 61 (2016) 199–206.
[158] E.P. Ivanova, J. Hasan, H.K. Webb, et al., Natural bactericidal surfaces: mechanical rupture of Pseudomonas aeruginosa cells by cicada wings, Small 8 (16) (2012) 2489–2494.
[159] G.S. Watson, D.W. Green, L. Schwarzkopf, et al., A gecko skin micro/nano structure – a low adhesion, superhydrophobic, anti-wetting, self-cleaning, biocompatible, antibacterial surface, Acta Biomater. 21 (2015) 109–122.
[160] J. Ma, Y. Sun, K. Gleichauf, et al., Nanostructure on taro leaves resists fouling by colloids and bacteria under submerged conditions, Langmuir 27 (16) (2011) 10035–10040.
[161] A. Elbourne, R.J. Crawford, E.P. Ivanova, Nano-structured antimicrobial surfaces: from nature to synthetic analogues, J. Colloid Interface Sci. 508 (2017) 603–616.
[162] S. Pogodin, J. Hasan, Vladimir A. Baulin, et al., Biophysical model of bacterial cell interactions with nanopatterned cicada wing surfaces, Biophys. J. 104 (4) (2013) 835–840.
[163] S.M. Kelleher, O. Habimana, J. Lawler, et al., Cicada wing surface topography: an investigation into the bactericidal properties of nanostructural features, ACS Appl. Mater. Interfaces 8 (24) (2015) 14966–14974.
[164] E.P. Ivanova, J. Hasan, H.K. Webb, et al., Bactericidal activity of black silicon, Nat. Commun. 4 (2013) 2838.
[165] D.E. Mainwaring, S.H. Nguyen, H. Webb, et al., The nature of inherent bactericidal activity: insights from the nanotopology of three species of dragonfly, Nanoscale 8 (12) (2016) 6527–6534.
[166] J. Hasan, H.K. Webb, V.K. Truong, et al., Spatial variations and temporal metastability of the self-cleaning and superhydrophobic properties of damselfly wings, Langmuir 28 (50) (2012) 17404–17409.
[167] V.K. Truong, N.M. Geeganagamage, V.A. Baulin, et al., The susceptibility of Staphylococcus aureus CIP 65.8 and Pseudomonas aeruginosa ATCC 9721 cells to the bactericidal action of nanostructured calopteryx haemorrhoidalis damselfly wing surfaces, Appl. Microbiol. Biotechnol. 101 (11) (2017) 4683–4690.
[168] R. Jiang, L. Hao, L. Song, et al., Lotus-leaf-inspired hierarchical structured surface with non-fouling and mechanical bactericidal performances, Chem. Eng. J. 398 (2020) 125609.
[169] J.V. Wandiyanto, T. Tamanna, D.P. Linklater, et al., Tunable morphological changes of asymmetric titanium nanosheets with bactericidal properties, J. Colloid Interface Sci. 560 (2020) 572–580.
[170] F. Viela, I. Navarro-Baena, J.J. Hernández, et al., Moth-eye mimetic cytocompatible bactericidal nanotopography: a convergent design, Bioinspiration Biomim. 13 (2) (2018) 026011.
[171] M.N. Dickson, E.I. Liang, L.A. Rodriguez, et al., Nanopatterned polymer surfaces with bactericidal properties, Biointerphases 10 (2) (2015) 021010.
[172] X. Li, Bactericidal mechanism of nanopatterned surfaces, Phys. Chem. Chem. Phys. 18 (2) (2016) 1311–1316.
[173] J. Ye, B. Li, Y. Zheng, et al., Eco-friendly bacteria-killing by nanorods through mechano-puncture with top selectivity, Bioact. Mater. 15 (2022) 173–184.
[174] L. Peng, H. Zhu, H. Wang, et al., Hydrodynamic tearing of bacteria on nanotips for sustainable water disinfection, Nat. Commun. 14 (1) (2023) 5734.
[175] S.K. Park, S.Y. Lee, S.B. Kim, et al., Dual-action antibacterial nanoblades for rapid inactivation of bioaerosols in personal protective equipment, Adv. Func. Mater. (2025) 2421728.
[176] J. Hasan, R.J. Crawford, E.P. Ivanova, Antibacterial surfaces: the quest for a new generation of biomaterials, Trends Biotechnol. 31 (5) (2013) 295–304.
[177] D.H.K. Nguyen, V.T.H. Pham, M. Al Kobaisi, et al., Adsorption of human plasma albumin and fibronectin onto nanostructured black silicon surfaces, Langmuir 32 (41) (2016) 10744–10751.
[178] V.T.H. Pham, V.K. Truong, A. Orlowska, et al., Race for the surface: Eukaryotic cells can win, ACS Appl. Mater. Interfaces 8 (34) (2016) 22025–22031.
[179] L. Zhao, T. Liu, X. Li, et al., Low-temperature hydrothermal synthesis of novel 3D hybrid nanostructures on titanium surface with mechano-bactericidal performance, ACS Biomater. Sci. Eng. 7 (6) (2021) 2268–2278.
[180] J. Hasan, K. Chatterjee, Recent advances in engineering topography mediated antibacterial surfaces, Nanoscale 7 (38) (2015) 15568–15575.
[181] J. Ye, J. Deng, Y. Chen, et al., Cicada and catkin inspired dual biomimetic antibacterial structure for the surface modification of implant material, Biomater. Sci. 7 (7) (2019) 2826–2832.
[182] T.L. Clainche, D. Linklater, S. Wong, et al., Mechano-bactericidal titanium surfaces for bone tissue engineering, ACS Appl. Mater. Interfaces 12 (43) (2020) 48272–48283.
[183] X. Luo, S. Yao, H. Zhang, et al., Biocompatible nano-ripples structured surfaces induced by femtosecond laser to rebel bacterial colonization and biofilm formation, Opt. Laser Technol. 124 (2020) 105973.
[184] S. Mo, K. Tang, Q. Liao, et al., Tuning the arrangement of lamellar nanostructures: achieving the dual function of physically killing bacteria and promoting osteogenesis, Mater. Horiz. 10 (3) (2023) 881–888.
[185] T. Wei, Z. Tang, Q. Yu, et al., Smart antibacterial surfaces with switchable bacteria-killing and bacteria-releasing capabilities, ACS Appl. Mater. Interfaces 9 (43) (2017) 37511–37523.
[186] Y. Zou, Y. Zhang, Q. Yu, et al., Dual-function antibacterial surfaces to resist and kill bacteria: painting a picture with two brushes simultaneously, J. Mater. Sci. Technol. 70 (2021) 24–38.
[187] Y. Chen, J. Gao, J. Ao, et al., Bioinspired nanoflakes with antifouling and mechano-bactericidal capacity, Colloids Surf. B Biointerfaces 224 (2023) 113229.
[188] L. Hao, R. Jiang, J. Gao, et al., Metal-organic framework (mof)-based slippery liquid-infused porous surface (slips) for purely physical antibacterial applications, Appl Mater. Today 27 (2022) 101430.
[189] R. Jiang, Y. Yi, L. Hao, et al., Thermoresponsive nanostructures: from mechano-bactericidal action to bacteria release, ACS Appl. Mater. Interfaces 13 (51) (2021) 60865–60877.
[190] Y. Yi, R. Jiang, Z. Liu, et al., Bioinspired nanopillar surface for switchable mechano-bactericidal and releasing actions, J. Hazard. Mater. 432 (2022) 128685.
[191] Z. Liu, Y. Yi, L. Song, et al., Biocompatible mechano-bactericidal nanopatterned surfaces with salt-responsive bacterial release, Acta Biomater. 141 (2022) 198–208.
[192] L.E. Fisher, Y. Yang, M.-F. Yuen, et al., Bactericidal activity of biomimetic diamond nanocone surfaces, Biointerphases 11 (1) (2016).
[193] A. Velic, J. Hasan, Z. Li, et al., Mechanics of bacterial interaction and death on nanopatterned surfaces, Biophys. J. 120 (2) (2021) 217–231.
[194] N. Lin, P. Berton, C. Moraes, et al., Nanodarts, nanoblades, and nanospikes: mechano-bactericidal nanostructures and where to find them, Adv. Colloid Interface Sci. 252 (2018) 55–68.
[195] S. Ishantha Senevirathne, J. Hasan, A. Mathew, et al., Trends in bactericidal nanostructured surfaces: an analytical perspective, ACS Appl. Bio Mater. 4 (10) (2021) 7626–7642.
[196] J. Hasan, H.K. Webb, V.K. Truong, et al., Selective bactericidal activity of nanopatterned superhydrophobic cicada psaltoda claripennis wing surfaces, Appl. Microbiol. Biotechnol. 97 (20) (2012) 9257–9262.
[197] F. Xue, J. Liu, L. Guo, et al., Theoretical study on the bactericidal nature of nanopatterned surfaces, J. Theor. Biol. 385 (2015) 1–7.
[198] J.-W. Xu, K. Yao, Z.-K. Xu, Nanomaterials with a photothermal effect for antibacterial activities: an overview, Nanoscale 11 (18) (2019) 8680–8691.
[199] J. Huo, Q. Jia, H. Huang, et al., Emerging photothermal-derived multimodal synergistic therapy in combating bacterial infections, Chem. Soc. Rev. 50 (15) (2021) 8762–8789.
[200] Y. Wang, H. Zhang, Z. Wang, et al., Photothermal conjugated polymers and their biological applications in imaging and therapy, ACS Appl. Polym. Mater. 2 (10) (2020) 4222–4240.
[201] W.-Y. Pan, C.-C. Huang, T.-T. Lin, et al., Synergistic antibacterial effects of localized heat and oxidative stress caused by hydroxyl radicals mediated by graphene/iron oxide-based nanocomposites, Nanomed. Nanotechnol. Biol. Med. 12 (2) (2016) 431–438.
[202] D. Jaque, L. Martínez Maestro, B. del Rosal, et al., Nanoparticles for photothermal therapies, Nanoscale 6 (16) (2014) 9494–9530.

[203] Y. Yang, L. Ma, C. Cheng, et al., Nonchemotherapic and robust dual-responsive nanoagents with on-demand bacterial trapping, ablation, and release for efficient wound disinfection, Adv. Funct. Mater. 28 (21) (2018).
[204] K.W. Tan, C.M. Yap, Z. Zheng, et al., State-of-the-art advances, development, and challenges of metal oxide semiconductor nanomaterials for photothermal solar steam generation, Adv. Sustain. Syst. 6 (4) (2022) 2100416.
[205] X. He, H. Wu, Y. Wang, et al., Bimodal antimicrobial surfaces of phytic acid-prussian blue nanoparticles-cationic polymer networks, Adv. Sci. 10 (16) (2023) e2300354.
[206] G. Guan, K.Y. Win, X. Yao, et al., Plasmonically modulated gold nanostructures for photothermal ablation of bacteria, Adv. Healthc. Mater. 10 (3) (2021) e2001158.
[207] S. Yougbare, C. Mutalik, D.I. Krisnawati, et al., Nanomaterials for the photothermal killing of bacteria, Nanomaterials 10 (6) (2020).
[208] X. Cui, Q. Ruan, X. Zhuo, et al., Photothermal nanomaterials: a powerful light-to-heat converter, Chem. Rev. 123 (11) (2023) 6891–6952.
[209] Y. Shi, M. Liu, F. Deng, et al., Recent progress and development on polymeric nanomaterials for photothermal therapy: a brief overview, J. Mater. Chem. B 5 (2) (2017) 194–206.
[210] A. D'Agostino, A. Taglietti, R. Desando, et al., Bulk surfaces coated with triangular silver nanoplates: antibacterial action based on silver release and photo-thermal effect, Nanomaterials 7 (1) (2017) 7.
[211] Y.Q. Zhao, Y. Sun, Y. Zhang, et al., Well-defined gold nanorod/polymer hybrid coating with inherent antifouling and photothermal bactericidal properties for treating an infected hernia, ACS Nano 14 (2) (2020) 2265–2275.
[212] M. Han, X. Li, S. Shi, et al., Thermal control of photothermal implants inspired by polar bear skin for the treatment of infected bone defects, Mater. Horiz. 11 (19) (2024) 4651–4664.
[213] M. Xing, W. Qian, K. Ye, et al., All-in-one design of titanium-based dental implant systems for enhanced soft and hard tissue integration, Biomaterials 320 (2025) 123251.
[214] T. Kotnik, W. Frey, M. Sack, et al., Electroporation-based applications in biotechnology, Trends Biotechnol. 33 (8) (2015) 480–488.
[215] T.Y. Tsong, Electroporation of cell membrane, Biophys. J. 60 (2) (1991) 297–306.
[216] Z.Y. Huo, X. Xie, T. Yu, et al., Nanowire-modified three-dimensional electrode enabling low-voltage electroporation for water disinfection, Environ. Sci. Technol. 50 (14) (2016) 7641–7649.
[217] Z.-Y. Huo, Y. Luo, X. Xie, et al., Carbon-nanotube sponges enabling highly efficient and reliable cell inactivation by low-voltage electroporation, Environ. Sci. Nano 4 (10) (2017) 2010–2017.
[218] J. Lan, L. Xu, Y. Wu, et al., Refining and in-situ growth of polyaniline endows the cellulose fibers with electrical stimulation sterilization, Int. J. Biol. Macromol. 272 (2024) 132772.
[219] Y.-J. Kim, Z.-Y. Huo, X. Wang, et al., Walking-induced electrostatic charges enable in situ electroporated disinfection in portable water bottles, Nat. Water 2 (4) (2024) 360–369.
[220] Y.-W. Lu, Y. Wang, Y.-R. Liu, et al., Square-wave alternating voltage driving promotes nanowire-assisted electroporation inactivation and fouling resistance of pathogenic bacteria for water disinfection, Chem. Eng. J. 480 (2024).
[221] C.-M. Chiu, Y.-Y. Ke, T.-M. Chou, et al., Self-powered active antibacterial clothing through hybrid effects of nanowire-enhanced electric field electroporation and controllable hydrogen peroxide generation, Nano Energy 53 (2018) 1–10.
[222] Y. Yin, J. Ding, Y. Cao, et al., Electroporation effect of zno nanoarrays under low voltage for water disinfection, Nanotechnol. Rev. 12 (1) (2023).
[223] T.J. Piggot, D.A. Holdbrook, S. Khalid, Electroporation of the e. Coli and s. Aureus membranes: molecular dynamics simulations of complex bacterial membranes, J. Phys. Chem. B 115 (45) (2011) 13381–13388.
[224] Y. Yi, H. Dou, J. Zhao, et al., Low voltage-enhanced mechano-bactericidal biopatch, Nano Lett. 24 (49) (2024) 15806–15816.
[225] J. Tian, H. Feng, L. Yan, et al., A self-powered sterilization system with both instant and sustainable anti-bacterial ability, Nano Energy 36 (2017) 241–249.
[226] J. Li, X. Liu, L. Tan, et al., Zinc-doped prussian blue enhances photothermal clearance of Staphylococcus aureus and promotes tissue repair in infected wounds, Nat. Commun. 10 (1) (2019).
[227] X.D. Liu, B. Chen, G.G. Wang, et al., Controlled growth of hierarchical Bi2Se3/CdSe-Au nanorods with optimized photothermal conversion and demonstrations in photothermal therapy, Adv. Funct. Mater. 31 (43) (2021).
[228] X. Zhao, Z. Xu, Z. Wei, et al., Nature-inspired mechano-bactericidal nanostructured surfaces with photothermally enhanced antibacterial performances, Prog. Org. Coat. 182 (2023) 107599.
[229] J. Xu, Y. Zhao, Y. Chen, et al., A superhydrophilic, light/microwave-absorbing coating with remarkable antibacterial efficacy, ACS Appl. Mater. Interfaces 14 (37) (2022) 42468–42482.
[230] Y. Cai, L. Wang, H. Hu, et al., A synergistic antibacterial platform: combining mechanical and photothermal effects based on Van-MoS2–Au nanocomposites, Nanotechnology 32 (8) (2020) 085102.
[231] X. Zhang, J. Zhang, X. Han, et al., A photothermal therapy enhanced mechano-bactericidal hybrid nanostructured surface, J. Colloid Interface Sci. 645 (2023) 380–390.
[232] X. Zhang, G. Zhang, M. Chai, et al., Synergistic antibacterial activity of physical-chemical multi-mechanism by TiO2 nanorod arrays for safe biofilm eradication on implant, Bioact. Mater. 6 (1) (2021) 12–25.
[233] P.Y. Liu, Z.H. Miao, K. Li, et al., Biocompatible Fe(3+)-TA coordination complex with high photothermal conversion efficiency for ablation of cancer cells, Colloids Surf. B Biointerfaces 167 (2018) 183–190.
[234] T. Wang, D.K. Brown, X. Xie, Operando investigation of locally enhanced electric field treatment (LEEFT) harnessing lightning-rod effect for rapid bacteria inactivation, Nano Lett. 22 (2) (2021) 860–867.
[235] H. Liu, W. Huang, Y. Yu, et al., Lightning-rod effect on nanowire tips reinforces electroporation and electrochemical oxidation: an efficient strategy for eliminating intracellular antibiotic resistance genes, ACS Nano 17 (3) (2023) 3037–3046.
[236] M.T. Sim, Z.Y. Ee, Y.H. Lim, et al., Instant disinfecting face masks utilizing electroporation powered by respiration-driven triboelectric nanogenerators, Adv. Func. Mater. 34 (51) (2024) 2410062.
[237] Y. Yi, H. Dou, J. Li, et al., Bioinspired self-powered nanostructures for efficient antibacterial activities, Nano Energy 134 (2025) 110527.
[238] Y. Wang, K.-K. Liu, W.-B. Zhao, et al., Antibacterial fabrics based on synergy of piezoelectric effect and physical interaction, Nano Today 48 (2023) 101737.
[239] H. Fan, Z. Guo, Bioinspired surfaces with wettability: biomolecule adhesion behaviors, Biomater. Sci. 8 (6) (2020) 1502–1535.
[240] S. Yuan, S. Luan, S. Yan, et al., Facile fabrication of lubricant-infused wrinkling surface for preventing thrombus formation and infection, ACS Appl. Mater. Interfaces 7 (34) (2015) 19466–19473.
[241] X. Sheng, J. Zhang, Air layer on superhydrophobic surface underwater, Colloids Surf. A 377 (1-3) (2011) 374–378.
[242] Y.A. Mehanna, E. Sadler, R.L. Upton, et al., The challenges, achievements and applications of submersible superhydrophobic materials, Chem. Soc. Rev. 50 (11) (2021) 6569–6612.
[243] E.M. Domingues, S. Arunachalam, J. Nauruzbayeva, et al., Biomimetic coating-free surfaces for long-term entrapment of air under wetting liquids, Nat. Commun. 9 (1) (2018) 3606.
[244] Y. Zhang, Y. Hu, B. Xu, et al., Robust underwater air layer retention and restoration on salvinia-inspired self-grown heterogeneous architectures, ACS Nano 16 (2) (2022) 2730–2740.
[245] K. Xiao, X. Cao, X. Chen, et al., Bactericidal efficacy of nanopatterned surface tuned by topography, J. Appl. Phys. 128 (6) (2020).
[246] K. Modaresifar, S. Azizian, M. Ganjian, et al., Bactericidal effects of nanopatterns: a systematic review, Acta Biomater. 83 (2019) 29–36.
[247] J. Wang, P. Li, N. Wang, et al., Antibacterial features of material surface: strong enough to serve as antibiotics? J. Mater. Chem. B 11 (2) (2023) 280–302.
[248] Y. Chen, Y. Gao, Y. Chen, et al., Nanomaterials-based photothermal therapy and its potentials in antibacterial treatment, J. Control. Release 328 (2020) 251–262.
[249] B. Jia, X. Du, W. Wang, et al., Nanophysical antimicrobial strategies: a rational deployment of nanomaterials and physical stimulations in combating bacterial infections, Adv. Sci. 9 (10) (2022) e2105252.
[250] H. Li, C. Wang, H. Shi, Development of endolysin-integrated ph-responsive anti-adhesive and antibacterial coatings with nanorods for the prevention of cross-contamination in fresh produce, Food Res. Int. 202 (2025) 115762.
[251] Y. Liang, Y. Liang, H. Zhang, et al., Antibacterial biomaterials for skin wound dressing, Asian J. Pharm. Sci. 17 (3) (2022) 353–384.
[252] Y. Liu, B. Li, C. Yi, et al., Application of polydopamine as antibacterial and anti-inflammatory materials, Prog. Biomed. Eng. 7 (2) (2025).
[253] Y.-H. Chen, S.-W. Guan, M. Xing, et al., Ce-doped defective titanium oxide coating with antibacterial, antioxidant and anti-inflammatory properties for potential application of peri-implantitis treatment, Rare Met 44 (1) (2024) 472–488.
[254] Y. Zhang, J. Cui, K.Y. Chen, et al., A smart coating with integrated physical antimicrobial and strain-mapping functionalities for orthopedic implants, Sci. Adv. 9 (18) (2023) eadg7397.
[255] X. Zhao, T. Chen, J. Liu, et al., Development of antifouling antibacterial polylactic acid (PLA) -based packaging and application for chicken meat preservation, Food Chem. 463 (Pt 1) (2025) 141116.
[256] F. Li, Y. An, J. Xue, et al., Cellulose acetate membranes: antibacterial strategy and application-a review, Small 21 (5) (2025) e2409728.
[257] R. Tao, C. Wang, Y. Yang, et al., Breathable triboelectric textiles with high efficiency air filtration and rapid self-disinfection properties for bioprotection and wireless biosensing, Surf. Interfaces 62 (2025) 106203.
[258] N. Mp, B.M. Rao, Anodized cuo nanoflakes for the antibacterial and antifungal applications, Heliyon 11 (3) (2025) e42304.
[259] H.J. Ensikat, P. Ditsche-Kuru, C. Neinhuis, et al., Superhydrophobicity in perfection: the outstanding properties of the lotus leaf, Beilstein J. Nanotechnol. 2 (2011) 152–161.